



# Molecular Docking, ADMET & DFT Predictions of *Cinnamomum zylanicum* for Prostate Cancer Inhibition

Adindu Chinonso Blessing <sup>a\*</sup>, Kalu Georgina Ijeoma <sup>a</sup>,  
Ikezu Uju Paul J.M <sup>a</sup>, Ikpa Chinaka B. C. <sup>a</sup>  
and Okeke Pamela I <sup>b</sup>

<sup>a</sup> Department of Chemistry, Imo State University, P M B 2000, Owerri, Imo State, Nigeria.

<sup>b</sup> Department of Basic Science, Alvan Ikoku University of Education Owerri, Nigeria.

## Authors' contributions

This work was carried out in collaboration among all authors. All authors read and approved the final manuscript.

## Article Information

### Open Peer Review History:

This journal follows the Advanced Open Peer Review policy. Identity of the Reviewers, Editor(s) and additional Reviewers, peer review comments, different versions of the manuscript, comments of the editors, etc are available here: <https://www.sdiarticle5.com/review-history/120835>

Original Research Article

Received: 01/06/2024

Accepted: 03/08/2024

Published: 08/08/2024

## ABSTRACT

The prostate gland found in men helps in semen production. When the prostate gland enlarges out of control, it could lead to prostate cancer. *Cinnamomum zeylanicum* (CZ) is a flavouring plant that is used as spice in foods. Prostate cancer is one of the deadliest malignancies diagnosed in men. It is the third largest source of cancer-related mortalities across the globe. The anti-prostate properties of *Cinnamomum zeylanicum* were studied by molecular docking method. The chemical constituents of the plant were extracted in chloroform, Absorption, distribution, metabolism, elimination and toxicity (ADMET) Screening were done to predict the drug-like properties, pharmacokinetics, and pharmacodynamics parameters of the identified compounds. Molecular docking analysis was used to identify the compound with the lowest binding energy using

\*Corresponding author: Email: [blessingojiegbe@yahoo.com](mailto:blessingojiegbe@yahoo.com);

**Cite as:** Blessing, Adindu Chinonso, Kalu Georgina Ijeoma, Ikezu Uju Paul J.M, Ikpa Chinaka B. C., and Okeke Pamela I. 2024. "Molecular Docking, ADMET & DFT Predictions of *Cinnamomum Zylanicum* for Prostate Cancer Inhibition". *Journal of Materials Science Research and Reviews* 7 (3):392-426. <https://journaljmsrr.com/index.php/JMSRR/article/view/340>.

methyltrienolone as the control drug. Density functional theory was used to identify the relationship between the structures of the compounds and their chemical reactivity. the ADMET result showed that two of the compounds were carcinogens while twenty-nine of them are safe for human consumption. Copaene gave the lowest binding energy. The DFT results revealed that the compounds showed low energy gap between the LUMO and HOMO energies making the molecules reactive towards the drug target. The results showed that compounds contained in *Cinnamomum zeylanicum* are good drug lead candidates for prostate cancer inhibition.

**Keywords:** *Cinnamomum zeylanicum*; molecular docking; prostate cancer; methyltrienolone; copaene.

## 1. INTRODUCTION

The prostate is a small gland found in men, it forms part of the reproductive system since it helps in the production of semen. It gets enlarged as one grows old. Prostate cancer begins when the prostate cells grow out of control, it is a disease that affects men especially after the age of 40 [1-2]. One in every four men is known to suffer from prostate enlargement. It is one of the most rampant malignancies diagnosed in men around the globe [3-4]. Normal increase and preservation of the prostate is based on androgen hormones which act through the androgen receptor. Stimulating the androgen receptor triggers the formation of prostate cancer. Lately, interest has moved towards identifying dietary ingredients that could exert anti-carcinogenic effects on prostate cancer cells [5-6]. It has been shown that food materials containing flavonoids can constrain androgen receptors thereby inhibit the growth of prostate cancer cells [7-8].

*Cinnamomum zeylanicum* an indigenous tropical spice is found in every household used mainly for its flavoring purpose. It has some medicinal applications; it is a member of the Lauraceae family. It has been reported to have several health benefits [9] such as inhibition of cancer growth, blood sugar regulation, cholesterol reduction, anti-bacterial, anti-viral, anti-fungal, anti-oxidant and anti-inflammatory properties. [10-14].

Molecular docking is a procedure employed in drug discovery and formulation to identify the correct protein– ligand binding configurations. This method usually involves the binding of a molecule with the correct macromolecule and then tabulating the binding free energy for the ligand and receptor [15-18].

The present work tries to evaluate phytochemicals in *Cinnamomum zeylanicum* for their prostate cancer growth inhibiting activities.

## 2. MATERIALS AND METHODS

### 2.1 Preparation of the *Cinnamomum zeylanicum*

The *Cinnamomum zeylanicum* used in this study was harvested from a local farm in Imo state, dried and ground to powdered form, dipped in chloroform to extract its chemical constituents, filtered, concentrated and sent for FTIR and GC-MS analysis.

### 2.2 Identification of Phytochemicals

The prepared plant material was submitted for Fourier transform infrared spectroscopy (FTIR) and gas-chromatography mass spectrophotometry (GC-MS) analysis to identify the phytochemicals present. The FTIR examination was performed with SHIMADZU Model no 84008 at the National research institute, Zaria Kaduna State Nigeria [19]. GC-MS examination was performed at the Amadu Bello university research laboratory using Agilent 19091S-433UI GCMS model with parameters HP-5ms Ultra Inert 0 °C—325 °C (350 °C): 30 m x 250 µm x 0.25, the phytochemicals were then identified from the GC-MS result by comparing with the National Institute of Standards and Technology (NIST) mass spectral library [20].

### 2.3 Ligand Preparation

Three-dimensional structure-data files (SDF) of the compounds identified in the GC-MS analysis were downloaded from PubChem online software, minimized using the PyRx virtual screening tool at universal force of step 200, converted to Auto Dock ligands (pdbqt) [21] and used in the docking process.

### 2.4 Identification and Preparation of Protein Molecular Target

The three-dimensional (3D) structure of the human androgen receptor molecular target with

PDB identity (1e3g) was identified from literature [22-23] and downloaded from protein database (PDB). The target was prepared in discovery studio software by removing the crystallographic water particles and co-crystallized ligand and saved as protein data band file for use in the molecular docking analysis. The centre grid boxes used were center\_x = 6.47003187, center\_y = 26.0675727032 and center\_z = 13.6157461091 and size\_x = 59.2024760498, size\_y = 54.35525508 and size\_z = 68.9708935269. Fig. 1 shows the human androgen receptor molecular target with the active site amino acid residues.

## 2.5 Absorption, Distribution, Metabolism, Elimination and Toxicity (ADMET) Screening

Examination of drug-like properties, pharmacokinetics, and pharmacodynamics parameters of the identified compounds was done using ADMETSAR online software. The canonical smiles of the compounds were

obtained from PubChem software and submitted to ADMETSAR for the screening [24].

## 2.6 Molecular Docking

To identify the binding energies of the protein-ligand interaction, molecular docking was performed by binding the 3D structures of the identified compounds on the human androgen receptor (PDB:1e3g). The molecular docking was done using the Autodock Vina found in the PyRx molecular docking software [25]. The docking results (binding energies) were organized in excel spread sheet while the post-docking visualization of the ligand-target interactions were performed in the discovery studio software.

## 2.7 Density Functional Theory Calculations

Density functional theory calculations were undertaken using the acceryl density functional theory (DFT) electronic structure DMol3 programs imbedded in the Materials Studio 8.0 software from Acceryl.

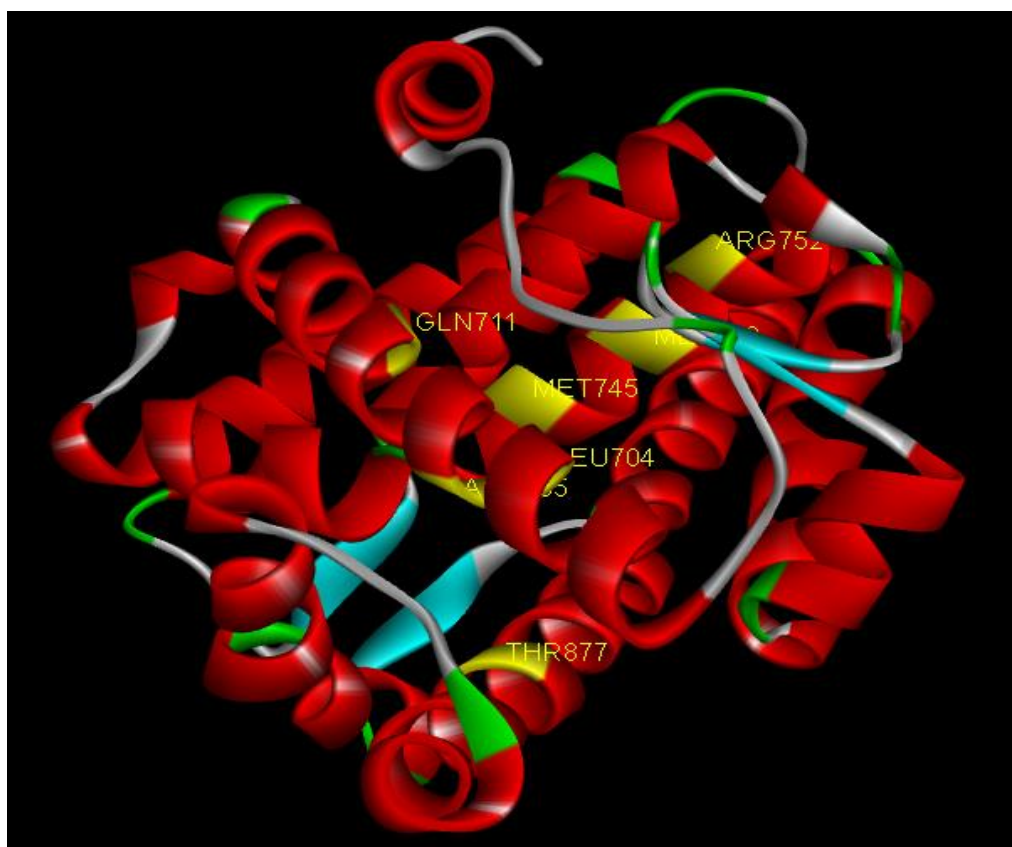


Fig. 1. The human androgen receptor molecular target (PDB: 1e3g ) with amino acid residues at the active site

### 3. RESULTS AND DISCUSSION

#### 3.1 Phytochemical Screening Results

FTIR analysis was undertaken on the plant material to identify the functional groups present. The spectrum is presented in Fig. 2. The prominent peaks observed in the spectrum include: 3343 cm<sup>-1</sup> corresponding to N-H bond,

2855.1 cm<sup>-1</sup>, 2922.2 cm<sup>-1</sup> of C-H bond, 16733.8 cm<sup>-1</sup>, 1729.5 cm<sup>-1</sup> of C=O and C=C respectively, 1449.9 cm<sup>-1</sup> C-H bond and 1124 cm<sup>-1</sup> of C-C bond.

The GC-MS analysis revealed 31 compounds which are listed in Table 1 while the chromatogram is shown in Fig. 3.

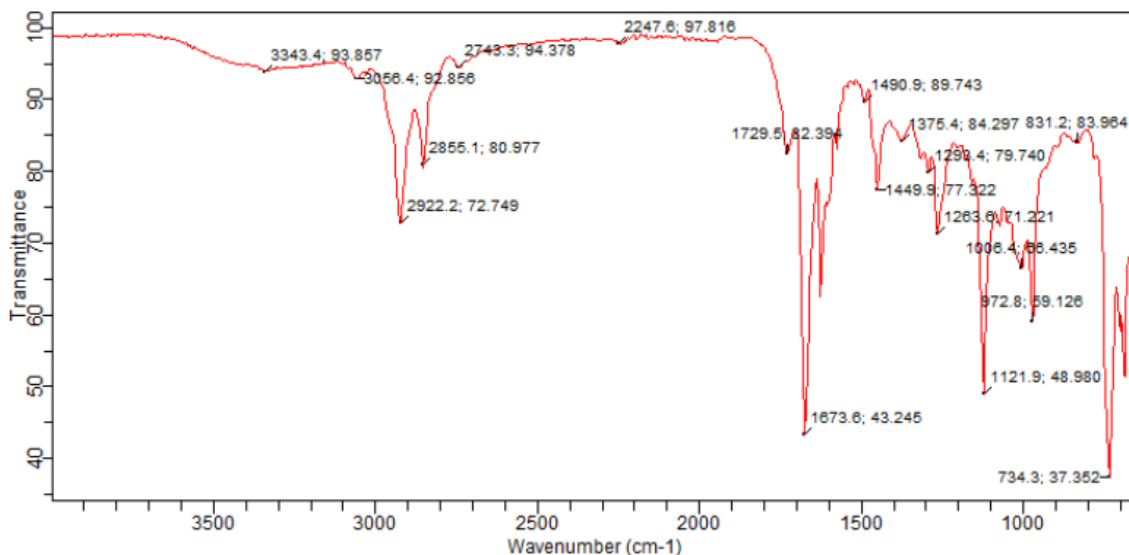


Fig. 2. FTIR spectrum of *Cinnamomum zeylanicum* powder

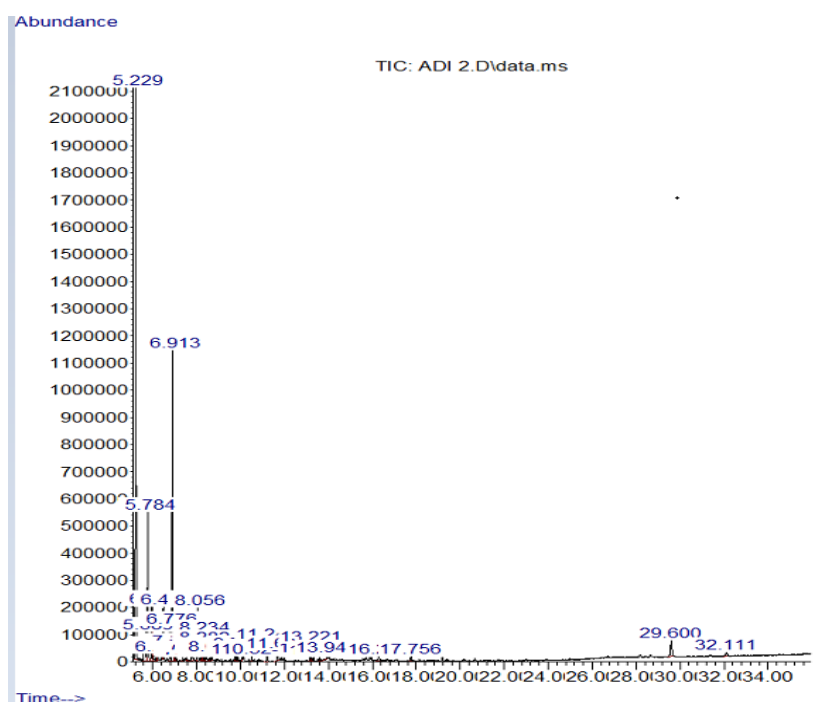
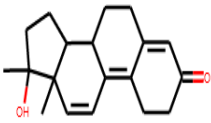
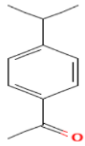
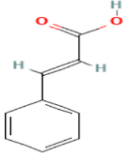
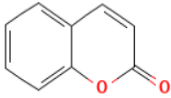
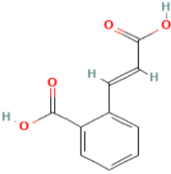
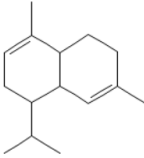
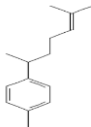
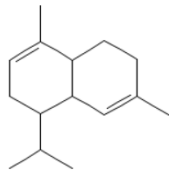
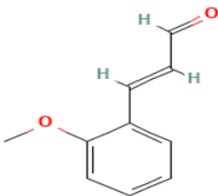
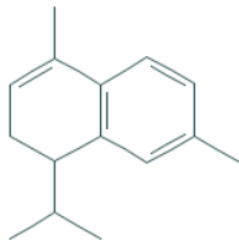
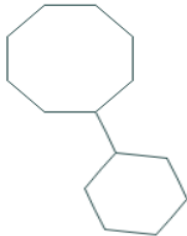
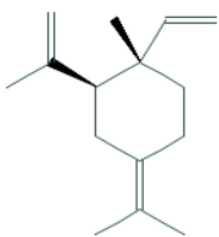
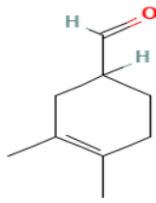
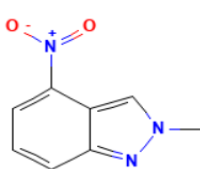
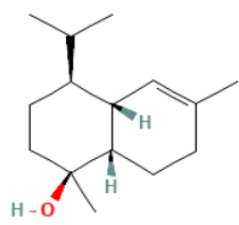
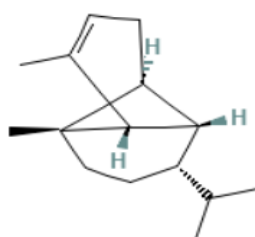
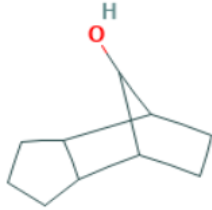
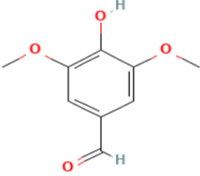
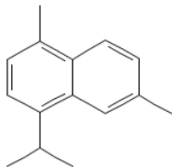
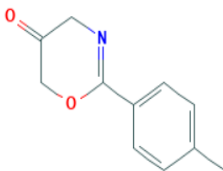
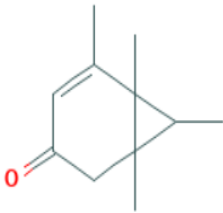
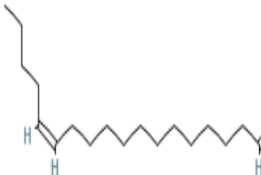

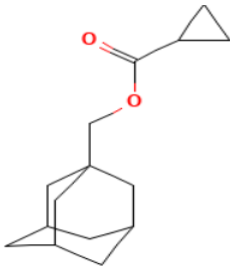


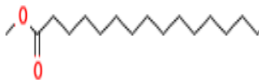


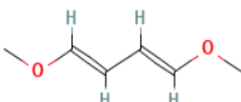
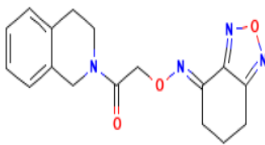
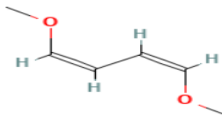
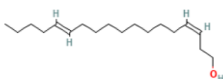
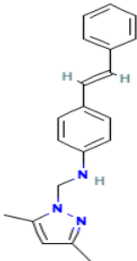
Fig. 3. GC-MS chromatogram of *Cinnamomum zeylanicum*

**Table 1. Compounds identified in the GC-MS analysis and Methyltrienolone as the control drug**

S.no	Compound	Area peak	Structure	Molecular formula	Molecular weight
1.	Methyltrienolone	Control		C <sub>19</sub> H <sub>24</sub> O <sub>2</sub>	284
2	Ethanone, 1-[4-(1-methylethyl)phenyl]-	38.3204		C <sub>11</sub> H <sub>14</sub> O	162.23
3	trans-Cinnamic acid	3.8033		C <sub>9</sub> H <sub>8</sub> O <sub>2</sub>	148.16
4	Coumarin	9.2153		C <sub>9</sub> H <sub>6</sub> O <sub>2</sub>	146.14
5	2-Carboxycinnamic acid	3.5487		C <sub>10</sub> H <sub>8</sub> O <sub>4</sub>	192.17
6	Naphthalene, 1,2,4a,5,6,8a-hexahydro-4,7-dimethyl-1-(1-methylethyl)-	0.5261		C <sub>15</sub> H <sub>24</sub>	204.35
7.	Benzene, 1-(1,5-dimethyl-4-hexenyl)-4-methyl-	0.4192		C <sub>15</sub> H <sub>22</sub>	202.33
8.	.alpha.-Muuroleone	5.564		C <sub>15</sub> H <sub>24</sub>	204.35
9.	2-Propenal, 3-(2-methoxyphenyl)-	20.4485		C <sub>10</sub> H <sub>10</sub> O <sub>2</sub>	162.18

10.	.alpha.-Calacorene	0.7418		C <sub>15</sub> H <sub>20</sub>	200.32
11.	Cyclooctane, cyclohexyl-	0.3927		C <sub>14</sub> H <sub>26</sub>	194.36
12.	Cyclohexane, 1-ethenyl-1-methyl-2-(1-methylethenyl)-4-(1-methylethylidene)-	0.245		C <sub>15</sub> H <sub>24</sub>	204.35
13.	3-Cyclohexen-1-carboxaldehyde, 3,4-dimethyl-	0.9413		C <sub>9</sub> H <sub>14</sub> O	138.21
14.	2H-Indazole, 2-methyl-4-nitro-	3.0644		C <sub>8</sub> H <sub>7</sub> N <sub>3</sub> O <sub>2</sub>	177.16
15.	.tau.-Muurolol	1.5205		C <sub>15</sub> H <sub>26</sub> O	222.37
16.	Copaene	0.9227		C <sub>15</sub> H <sub>24</sub>	204.35

17	Tricyclo[5.2.1.0 (2,6)]decan-10-ol	0.5396		C <sub>10</sub> H <sub>16</sub> O	152.23
18	Benzaldehyde, 4-hydroxy-3,5-dimethoxy-	0.2592		C <sub>9</sub> H <sub>10</sub> O <sub>4</sub>	182.17
19	Naphthalene, 1,6-dimethyl-4-(1-methylethyl)-	0.4642		C <sub>15</sub> H <sub>18</sub>	198.30
20	5,6-Dihydro-2-(4-tolyl)-4H-1,3-oxazin-5-one	0.4643		C <sub>11</sub> H <sub>11</sub> NO <sub>2</sub>	189.21
21	5,6,7,8-Tetramethylbicyclo[4.1.0]hept-4-en-3-one	0.5467		C <sub>11</sub> H <sub>16</sub> O	164.24
22	13-Octadecenal, (Z)-	0.3517		C <sub>18</sub> H <sub>34</sub> O	266.5
23	Tetradecanal	0.1483		C <sub>14</sub> H <sub>28</sub> O	212.37
24	Cyclopropanecarboxylic acid, (adamantanylmethyl) ester	0.2049		C <sub>15</sub> H <sub>22</sub> O <sub>2</sub>	234.33

25	Hexadecanoic acid, methyl ester	1.1074		C <sub>17</sub> H <sub>34</sub> O <sub>2</sub>	270.5
26	n-Hexadecanoic acid	0.7977		C <sub>16</sub> H <sub>32</sub> O <sub>2</sub>	256.42
27	13-Tetradecene-11-yn-1-ol	0.3584		C <sub>14</sub> H <sub>24</sub> O	208.34
28	1,3-Butadiene, 1,4-dimethoxy-, (E,E)-	1.3731		C <sub>6</sub> H <sub>10</sub> O <sub>2</sub>	114.14
29	2,1,3-Benzoxadiazol-4(5H)-one, 6,7-dihydro-, O-[2-[3,4-dihydro-2(1H)-isoquinolinyl]-2-oxoethyl]oxime	0.3090		C <sub>17</sub> H <sub>18</sub> N <sub>4</sub> O <sub>3</sub>	326.35
30	1,3-Butadiene, 1,4-dimethoxy-, (Z,Z)-	0.4579		C <sub>6</sub> H <sub>10</sub> O <sub>2</sub>	114.14
31	Z,E-3,13-Octadecadien-1-ol	0.3269		C <sub>18</sub> H <sub>34</sub> O	266.5
32	Benzenamine, 4-(2-phenylethenyl)-N-(3,5-dimethyl-1-pyrazolylmethyl)-	2.6169		C <sub>20</sub> H <sub>21</sub> N <sub>3</sub>	303.4

### 3.2 ADMET Result

Absorption, distribution, metabolism, elimination and toxicity examination was performed on the compounds. The ADMET properties showing their pharmacodynamics and pharmacokinetics are summarized in Table 2. Interestingly, none of the compounds violated more than one of the Lipinski's rule [26]. According to the rule an orally administered drug should not have more than 5 hydrogen bond donors, more than 10 hydrogen bond acceptors and should have a molecular

mass less than 500, Majority of the compounds show positive human intestine absorption indicating that they can be better taken from the gastrointestinal tract when consumed orally. Only two of the compounds were found to show carcinogenic properties. The blood brain barrier (BBB) penetration study was performed, the result indicated that four of the compounds gave negative result to penetrate blood brain; the obtained results indicated that the compounds could be a drug lead candidate.



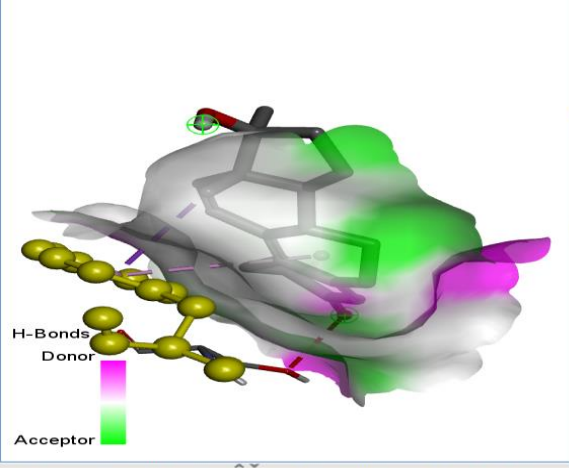
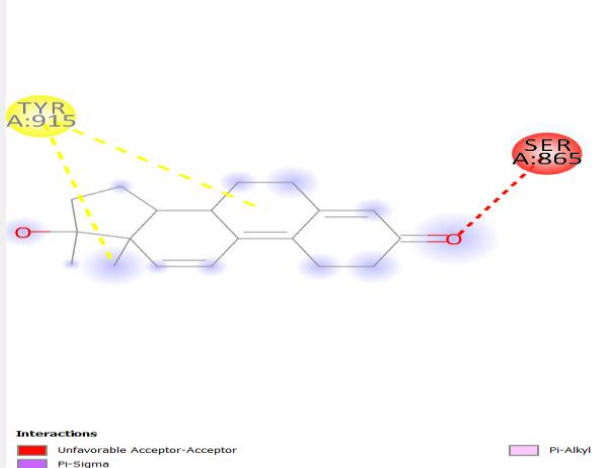
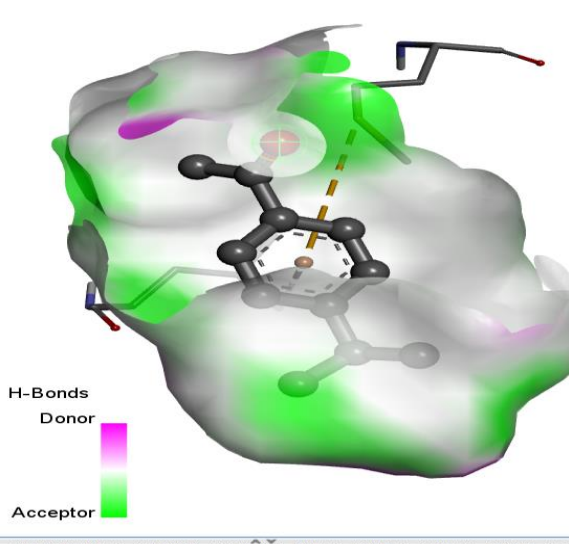
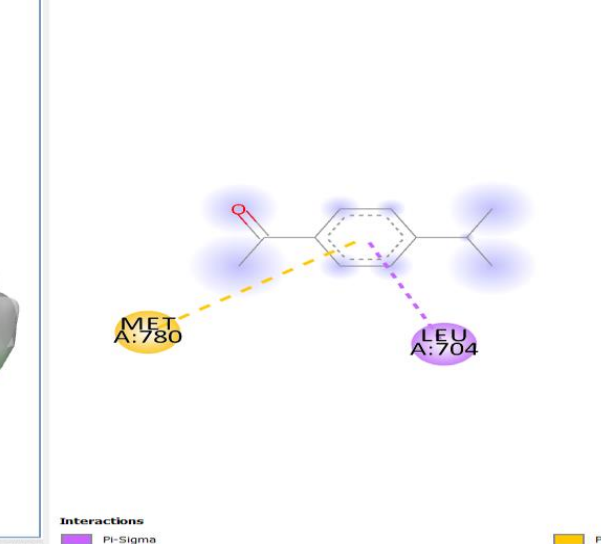
**Table 2. Absorption, distribution, metabolism, elimination and toxicity table**

s/no	Compound	HIA	BBB	H-bond acceptor	H-bond donor	Rotatable bonds	Carcinogenicity
1	Methyltrienolone	+	-	2	1	0	-
2	Ethanone, 1-[4-(1-methylethyl)phenyl]-	+	+	1	0	2	-
3	trans-Cinnamic acid	+	+	1	1	2	+
4	Coumarin	+	-	2	0	0	-
5	2-Carboxycinnamic acid	+	+	2	2	3	-
6	Naphthalene, 1,2,4a,5,6,8a-hexahydro-4,7-dimethyl-1-(1-methylethyl)-	+	+	0	0	1	-
7	Benzene, 1-(1,5-dimethyl-4-hexenyl)-4-methyl-	+	+	0	0	4	-
8	.alpha.-Muuroleone	+	+	0	0	1	-
9	2-Propenal, 3-(2-methoxyphenyl)-	+	-	2	0	3	-
10	.alpha.-Calacorene	+	+	0	0	1	-
11	Cyclooctane, cyclohexyl-	+	+	0	0	1	-
12	Cyclohexane, 1-ethenyl-1-methyl-2-(1-methylethenyl)-4-(1-methylethylidene)-	+	+	0	0	2	-
13	3-Cyclohexen-1-carboxaldehyde, 3,4-dimethyl-	+	+	1	0	1	-
14	2H-Indazole, 2-methyl-4-nitro-	+	+	4	0	1	-
15	.tau.-Muurolol	+	+	1	1	1	-
16	Copaene	+	+	0	0	1	-
17	Tricyclo[5.2.1.0 (2,6)]decan-10-ol	+	+	1	1	0	-
18	Benzaldehyde, 4-hydroxy-3,5-dimethoxy-	+	-	4	1	3	-
19	Naphthalene, 1,6-dimethyl-4-(1-methylethyl)-	+	+	0	0	1	-
20	5,6-Dihydro-2-(4-tolyl)-4H-1,3-oxazin-5-one	+	+	3	0	1	-
21	5,6,7,8-Tetramethylbicyclo[4.1.0]hept-4-en-3-one	+	+	1	0	0	-
22	13-Octadecenal, (Z)-	+	+	1	0	15	-
23	Tetradecanal	+	+	1	0	12	-
24	Cyclopropanecarboxylic acid, (adamantanyl-1)methyl ester	+	+	2	0	3	-
25	Hexadecanoic acid, methyl ester	+	+	2	0	14	-
26	n-Hexadecanoic acid	+	+	1	1	14	-
27	13-Tetradecene-11-yn-1-ol	+	+	1	1	9	-
28	1,3-Butadiene, 1,4-dimethoxy-, (E,E)-	+	+	2	0	3	+
28	2,1,3-Benzoxadiazol-4(5H)-one, 6,7-dihydro-, O-[2-[3,4-dihydro-2(1H)-isoquinoliny]-2-oxoethyl]oxime	+	+	6	0	3	-
30	1,3-Butadiene, 1,4-dimethoxy-, (Z,Z)-	+	+	2	0	3	-
31	Z,E-3,13-Octadecadien-1-ol	+	+	1	1	14	-
32	Benzenamine, 4-(2-phenylethenyl)-N-(3,5-dimethyl-1-pyrazolylmethyl)-	+	+	3	1	5	-

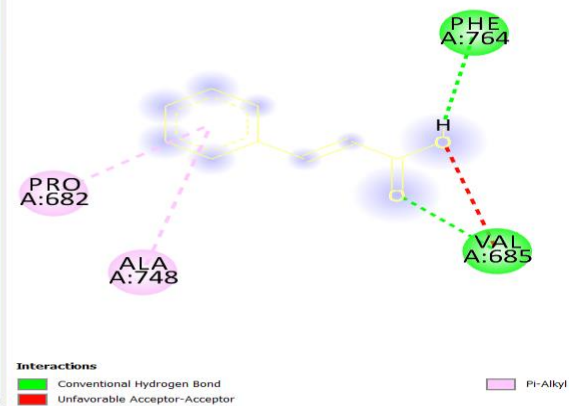
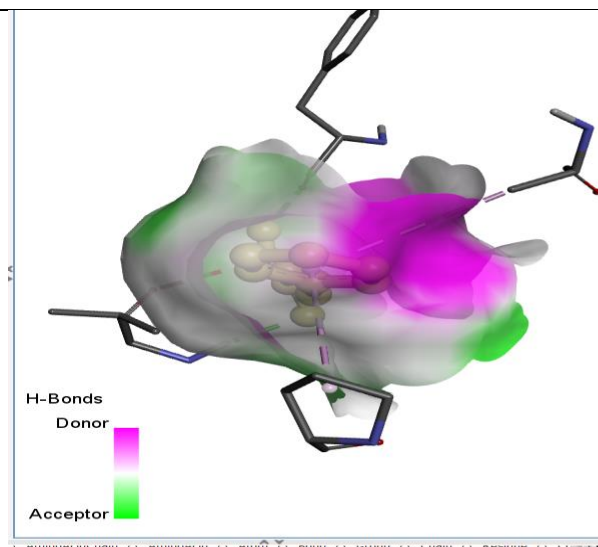
HIA=Human intestinal absorption, BBB= Blood Brain Barrier

**Table 3. Pubchem ID and DOCKING SCORES OF THE COMPOUNDS**

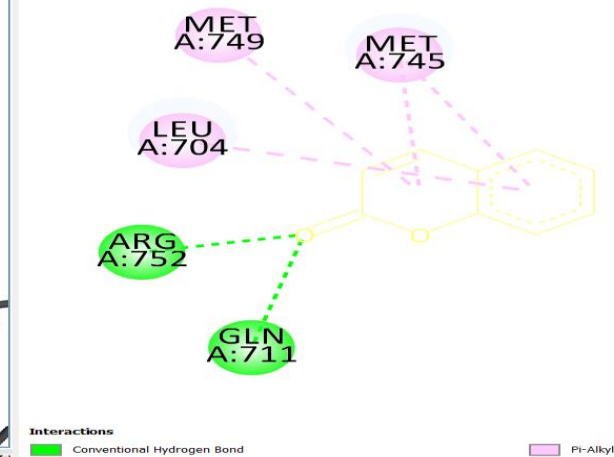
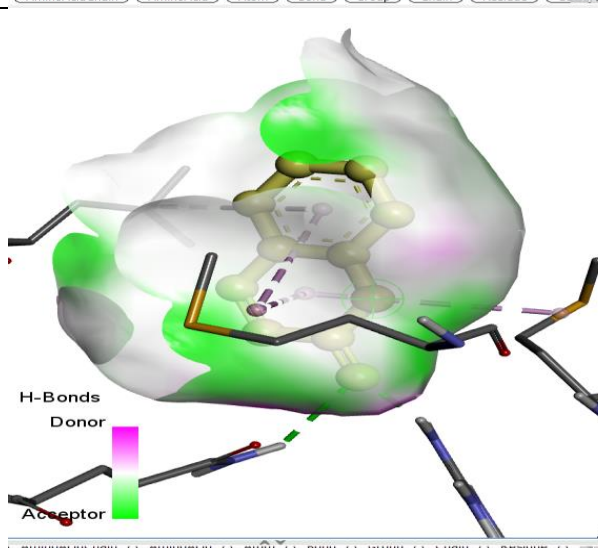
S/No.	Pubchem id	Name of compound	Docking score (kCal/mol)
1	261000	Methyltrienolone	-6.8
2	12578	Ethanone, 1-[4-(1-methylethyl)phenyl]-	-6.6
3	444539	trans-Cinnamic acid	-6.6
4	323	Coumarin	-7.0
5	904938	2-Carboxycinnamic acid	-7.1
6	101708	Naphthalene, 1,2,4a,5,6,8a-hexahydro-4,7-dimethyl-1-(1-methylethyl)-	-7.6
7	92139	Benzene, 1-(1,5-dimethyl-4-hexenyl)-4-methyl-	-6.6
8.	101708	.alpha.-Muuroloene	-7.1
9	641298	2-Propenal, 3-(2-methoxyphenyl)-	-6.0
10	528708	.alpha.-Calacorene	-7.6
11	543869	Cyclooctane, cyclohexyl-	-8.0
12	6432312	Cyclohexane, 1-ethenyl-1-methyl-2-(1-methylethenyl)-4-(1-methylethylidene)-	-7.6
13	537551	3-Cyclohexen-1-carboxaldehyde, 3,4-dimethyl-	-5.8
14	280212	2H-Indazole, 2-methyl-4-nitro-	-7.2
15	3084331	.tau.-Muurolol	-7.0
16	12303902	Copaene	-8.2
17	578081	Tricyclo[5.2.1.0 (2,6)]decan-10-ol	-6.3
18	8655	Benzaldehyde, 4-hydroxy-3,5-dimethoxy-	-5.7
19	10225	Naphthalene, 1,6-dimethyl-4-(1-methylethyl)-	-7.1
20	577139	5,6-Dihydro-2-(4-tolyl)-4H-1,3-oxazin-5-one	-7.8
21	578530	5,6,7,8-Tetramethylbicyclo[4.1.0]hept-4-en-3-one	-5.0
22	5364497	13-Octadecenal, (Z)-	-5.0
23	31291	Tetradecanal	-4.7
24	585226	Cyclopropanecarboxylic acid, (adamantanyl-1)methyl ester	-7.2
25	8181	Hexadecanoic acid, methyl ester	-5.2
26	985	n-Hexadecanoic acid	-4.7
27	543337	13-Tetradecene-11-yn-1-ol	-4.2
28	5362907	1,3-Butadiene, 1,4-dimethoxy-, (E,E)-	-3.9
29	9601008	2,1,3-Benzoxadiazol-4(5H)-one, 6,7-dihydro-, O-[2-[3,4-dihydro-2(1H)-isoquinolinyl]-2-oxoethyl]oxime	-7.1
30	5362908	1,3-Butadiene, 1,4-dimethoxy-, (Z,Z)-	-4.1
31	5364516	Z,E-3,13-Octadecadien-1-ol	-5.5
32	680405	Benzenamine, 4-(2-phenylethenyl)-N-(3,5-dimethyl-1-pyrazolylmethyl)-	-7.9

Name of compound	3D and 2D protein ligand interactions	
Methyltrienolone	3D	2D
<p data-bbox="181 331 405 368">Methyltrienolone</p>  <p data-bbox="741 660 831 703">H-Bonds Donor</p> <p data-bbox="741 767 831 788">Acceptor</p>	 <p data-bbox="1317 432 1391 469">TYR A:915</p> <p data-bbox="1816 469 1890 505">SER A:865</p> <p data-bbox="1317 762 1406 778"><b>Interactions</b></p> <p data-bbox="1361 778 1541 794">Unfavorable Acceptor-Acceptor</p> <p data-bbox="1361 794 1429 810">Pi-Sigma</p> <p data-bbox="1816 778 1899 794">Pi-Alkyl</p>	
<p data-bbox="181 810 674 847">Ethanone, 1-[4-(1-methylethyl)phenyl]-</p>  <p data-bbox="741 1198 831 1241">H-Bonds Donor</p> <p data-bbox="741 1321 831 1342">Acceptor</p>	 <p data-bbox="1420 1129 1494 1166">MET A:780</p> <p data-bbox="1711 1145 1785 1182">LEU A:704</p> <p data-bbox="1361 1331 1451 1347"><b>Interactions</b></p> <p data-bbox="1361 1347 1464 1362">Pi-Sigma</p> <p data-bbox="1861 1347 1951 1362">Pi-Sulfur</p>	

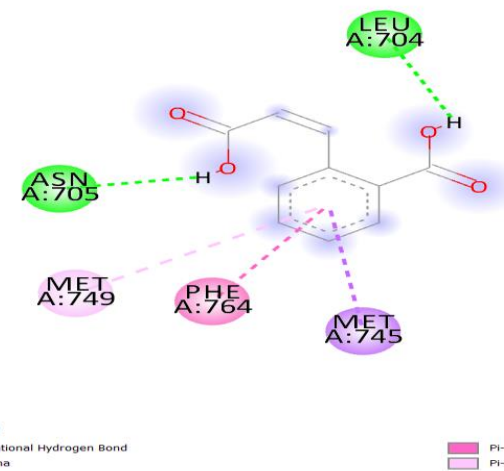
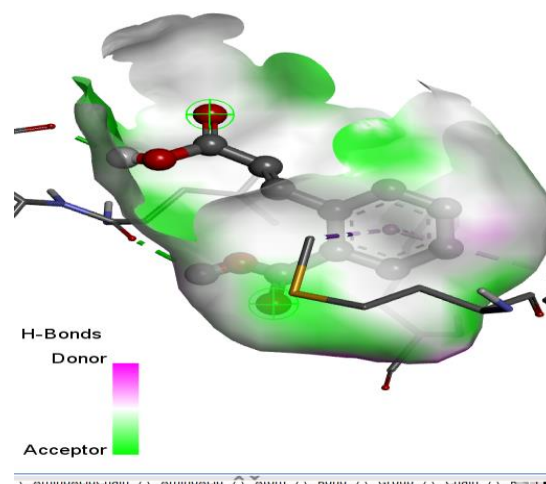
### trans-Cinnamic acid



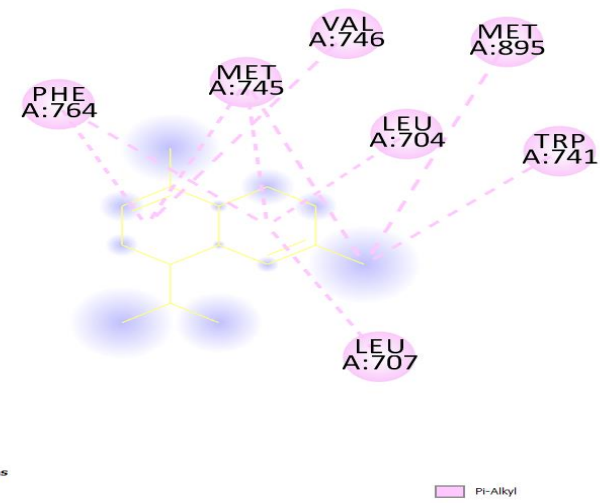
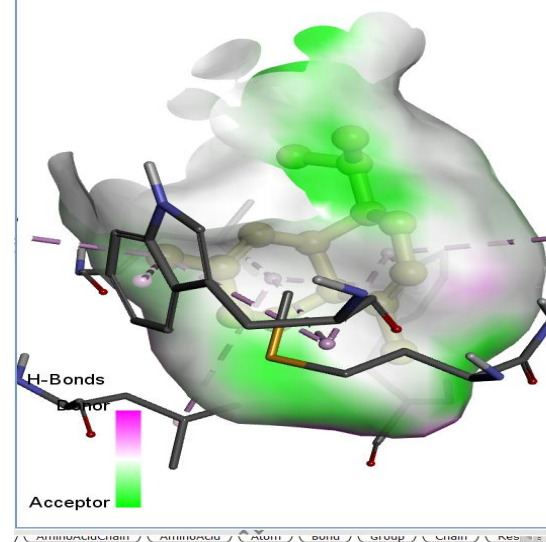
### Coumarin



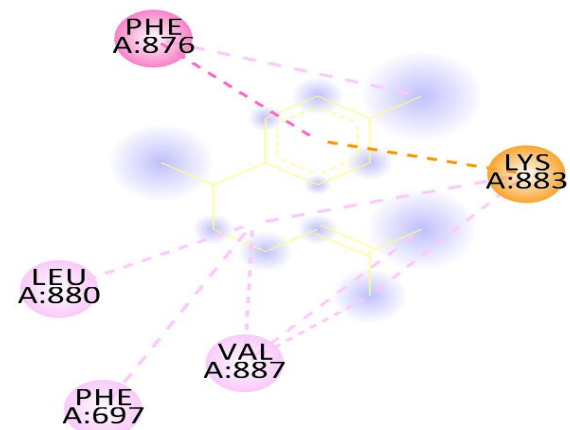
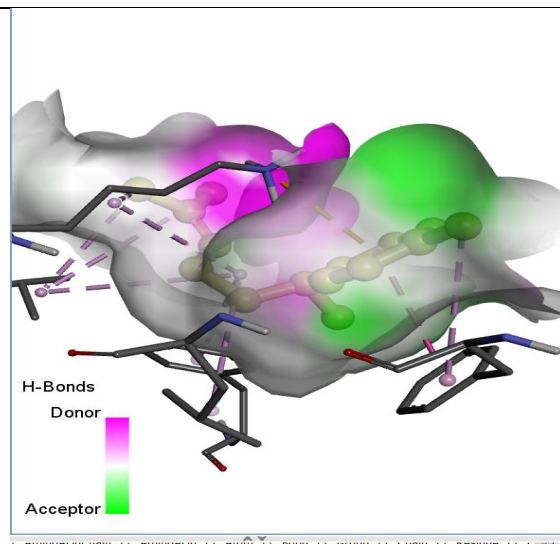
### 2-Carboxycinnamic acid



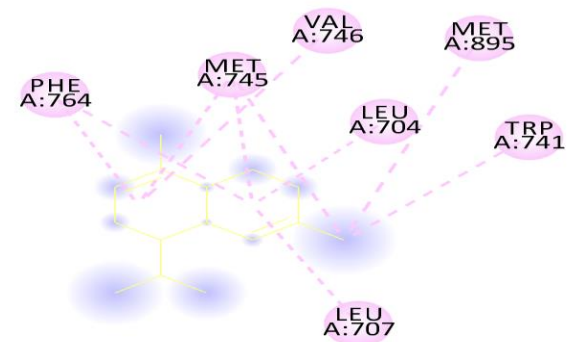
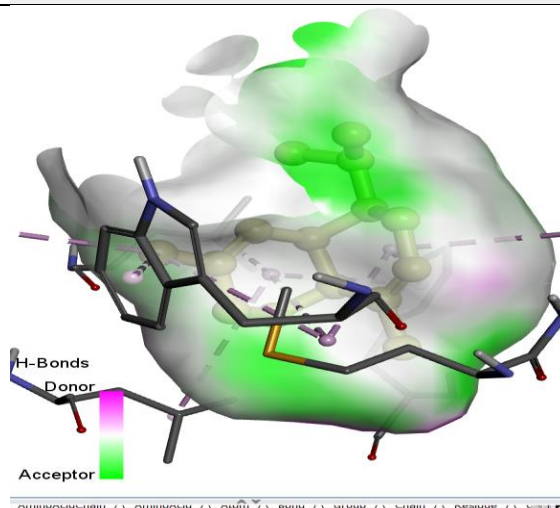
### Naphthalene, 1,2,4a,5,6,8a-hexahydro-4,7-dimethyl-1-(1-methylethyl)-



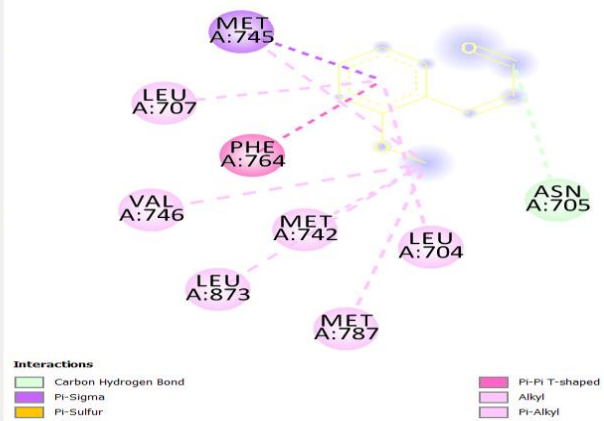
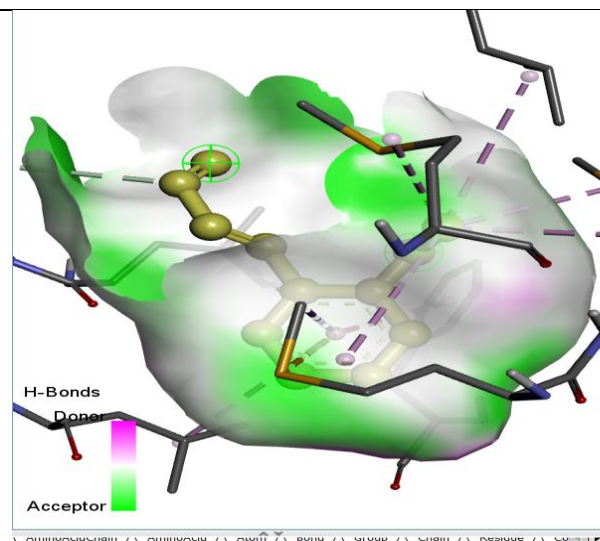
**Benzene, 1-(1,5-dimethyl-4-hexenyl)-4-methyl-**



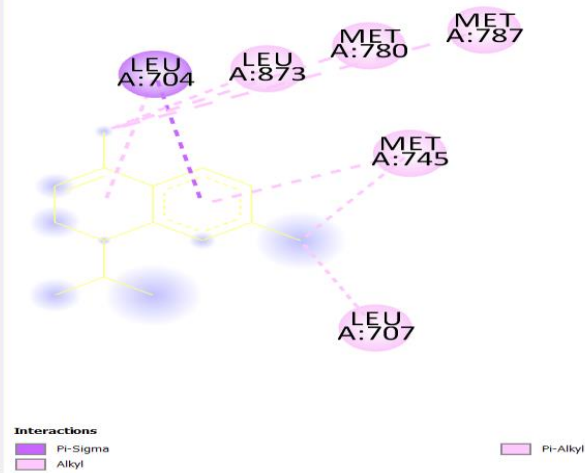
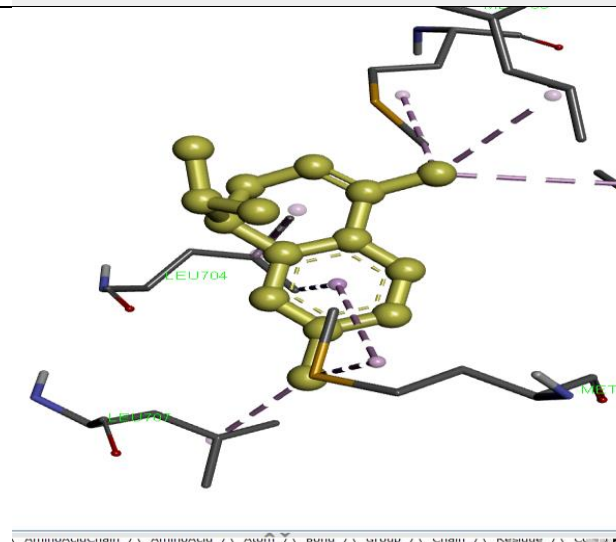
**.alpha.-Muurolene**



**2-Propenal, 3-(2-methoxyphenyl)-**

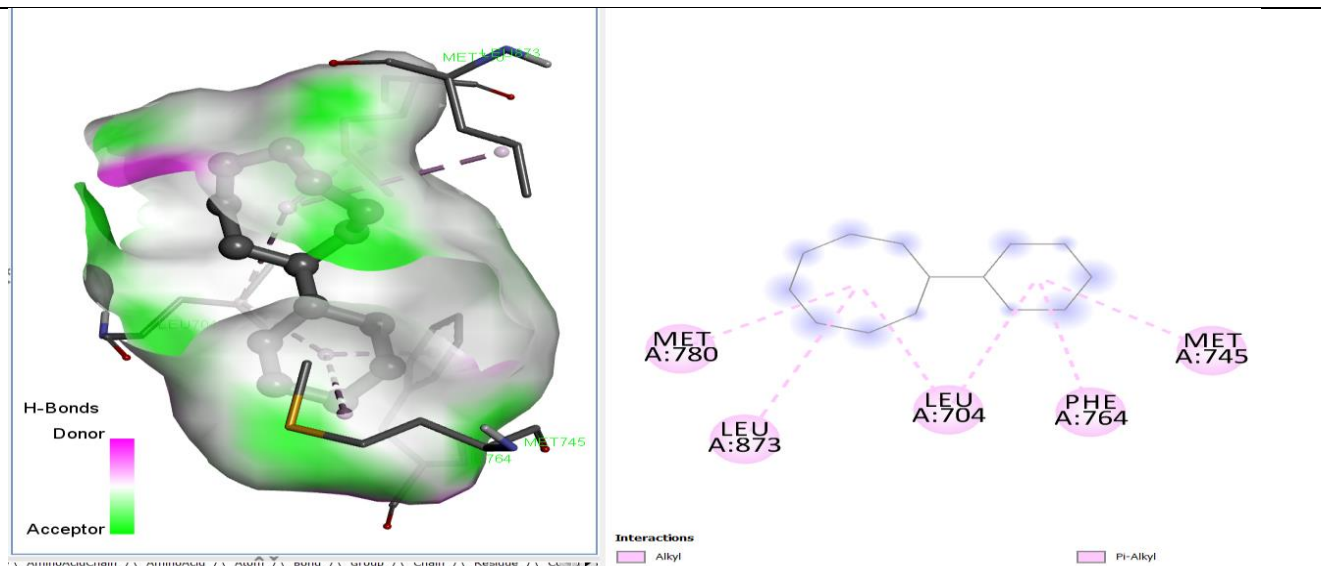


**.alpha.-Calacorene**

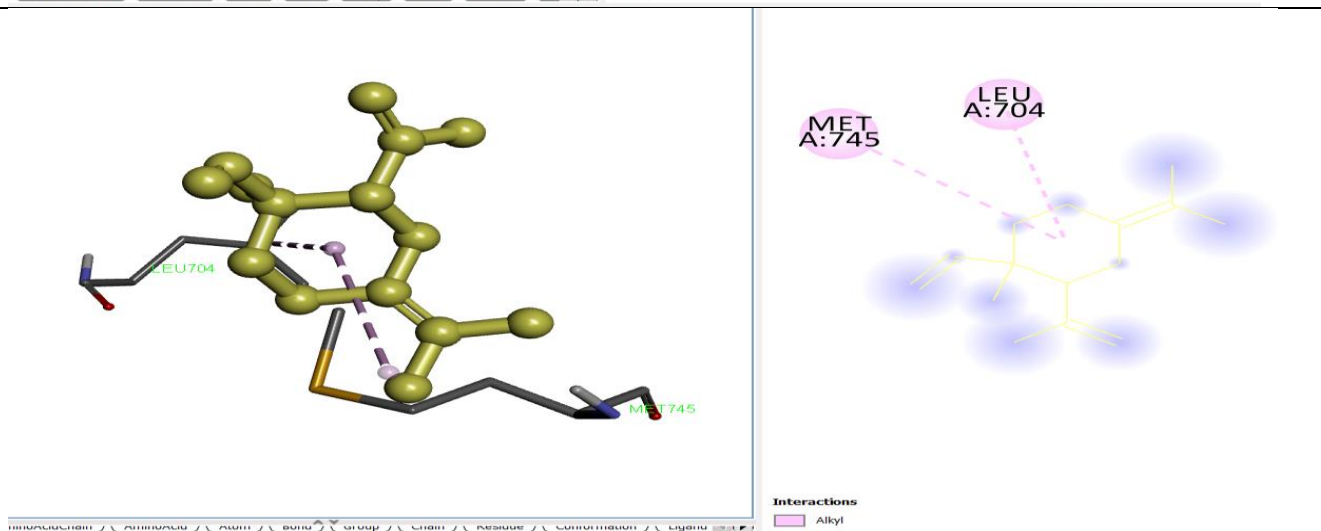




**Cyclooctane, cyclohexyl-**

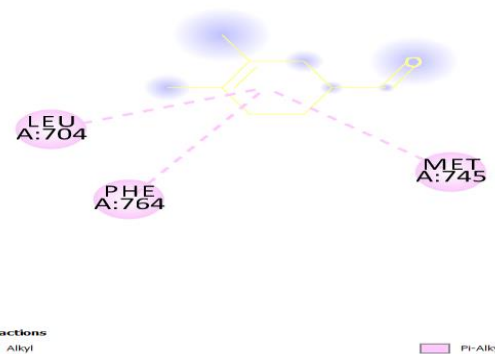
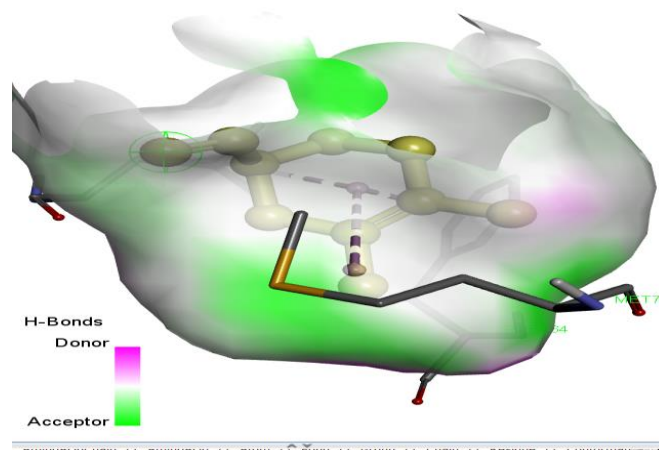


**Cyclohexane, 1-ethenyl-1-methyl-2-(1-methylethenyl)-4-(1-methylethylidene)-**

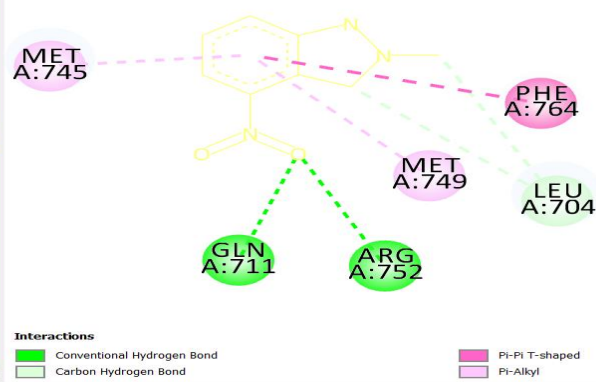
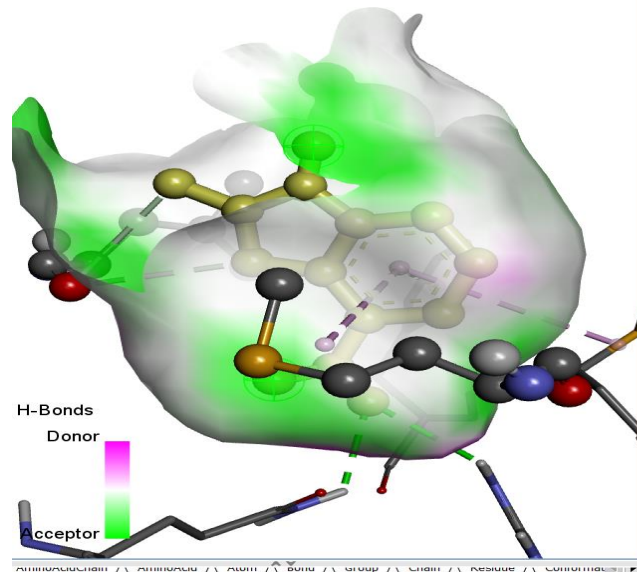




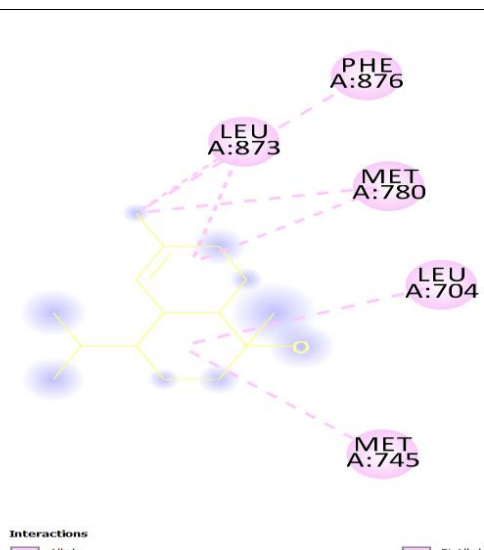
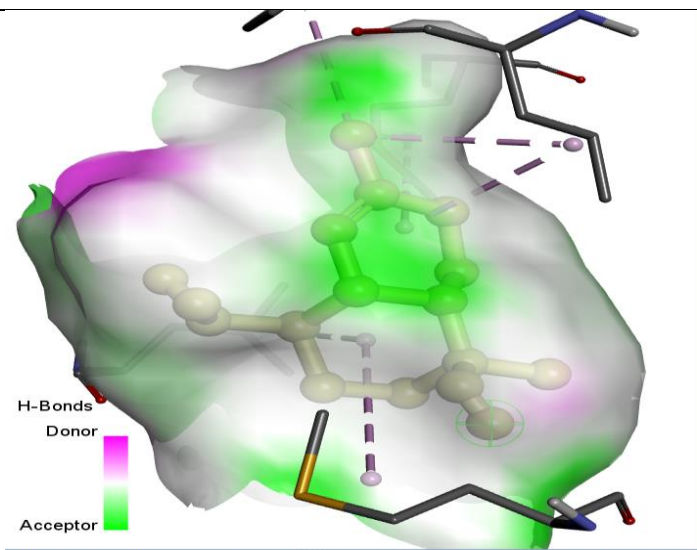
**3-Cyclohexen-1-carboxaldehyde, 3,4-dimethyl-**



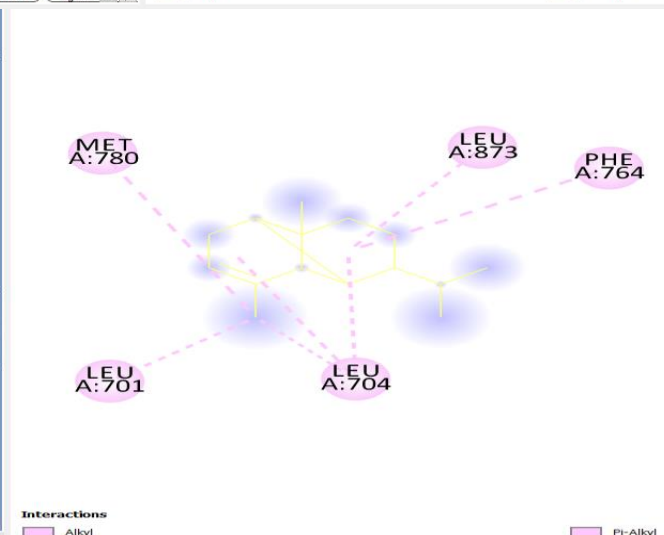
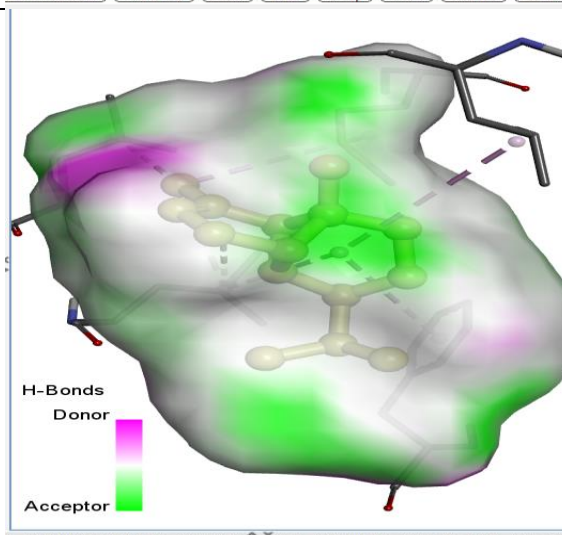
**2H-Indazole, 2-methyl-4-nitro-**



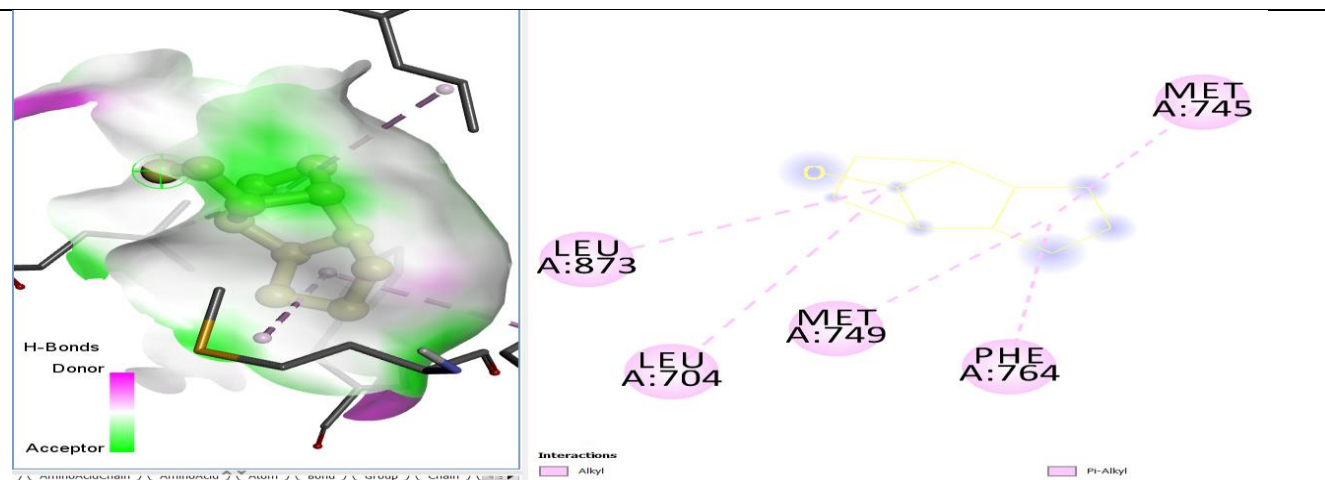
**.tau.-Muurolol**



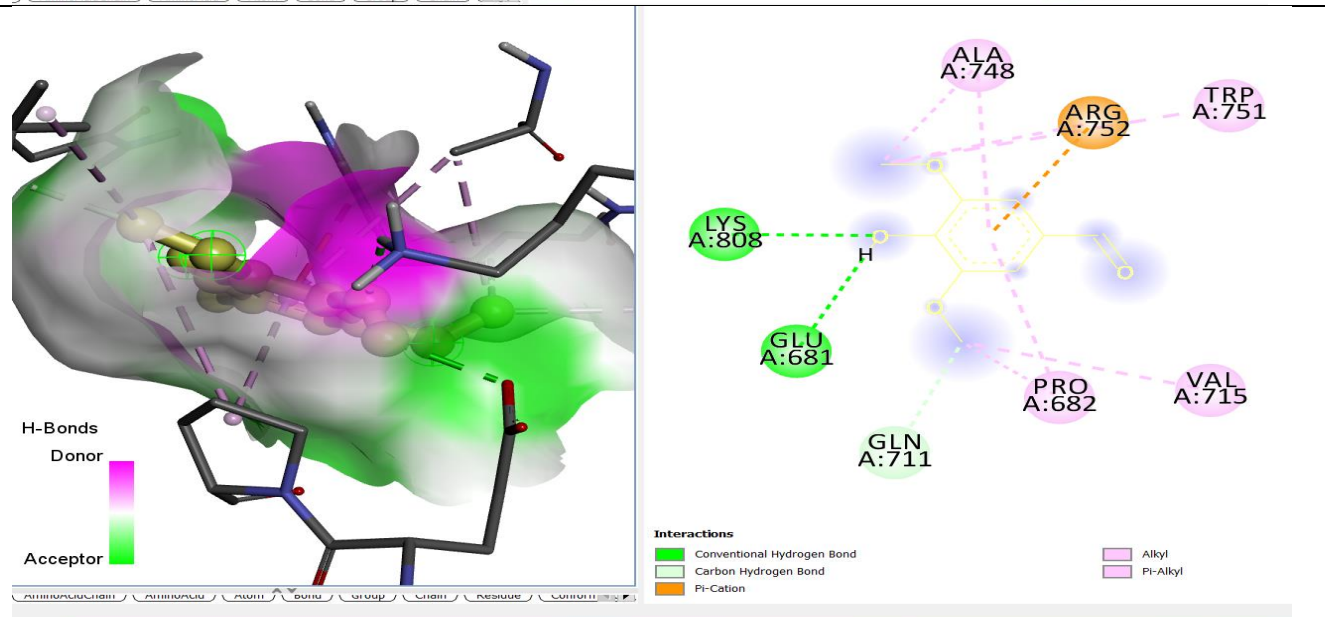
**Copaene**



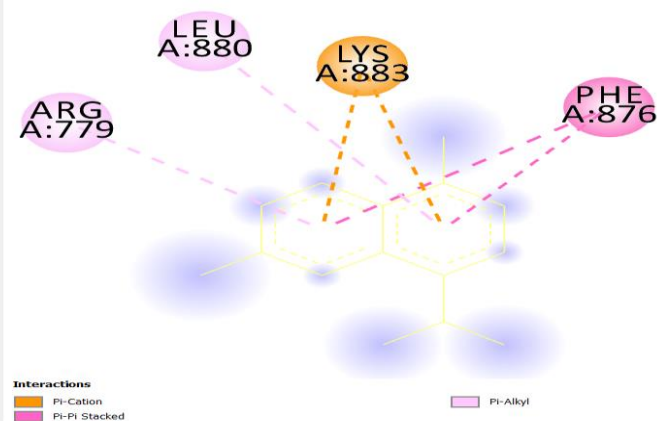
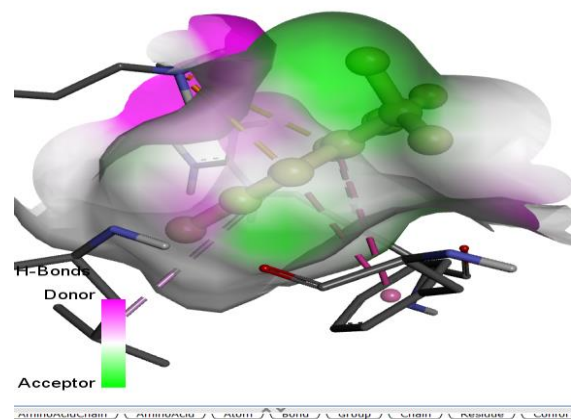
### Tricyclo[5.2.1.0 (2,6)]decan-10-ol



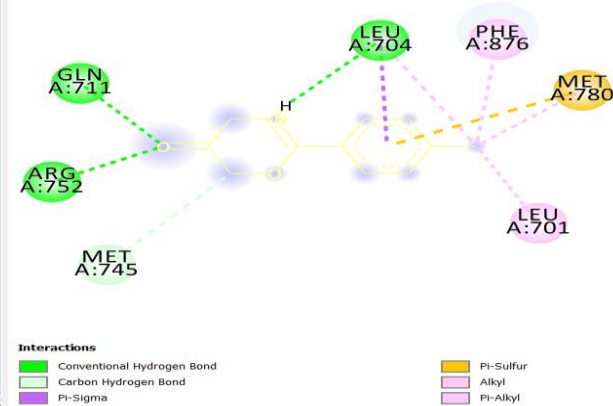
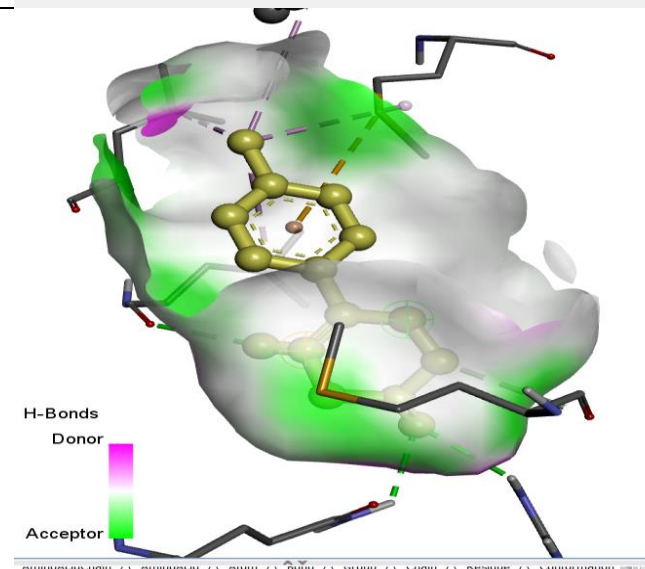
### Benzaldehyde, 4-hydroxy-3,5-dimethoxy-



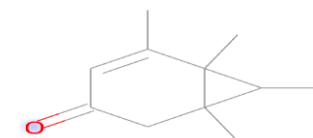
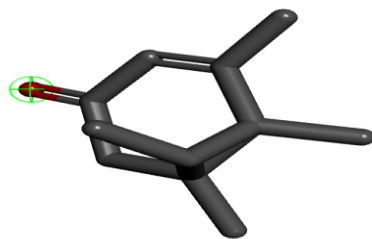
**Naphthalene, 1,6-dimethyl-4-(1-methylethyl)-**



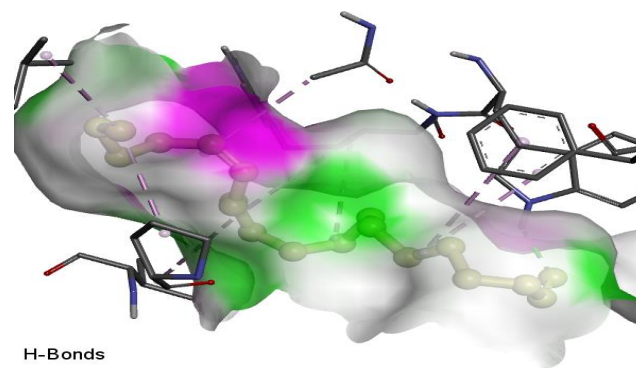
**5,6-Dihydro-2-(4-tolyl)-4H-1,3-oxazin-5-one**



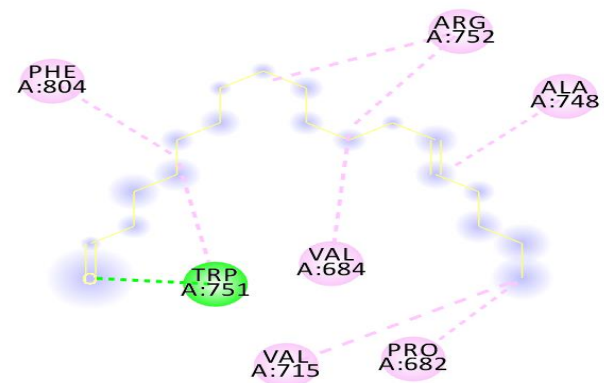
5,6,7,8-Tetramethylbicyclo[4.1.0]hept-4-en-3-one



13-Octadecenal, (Z)-



H-Bonds  
Donor  
Acceptor

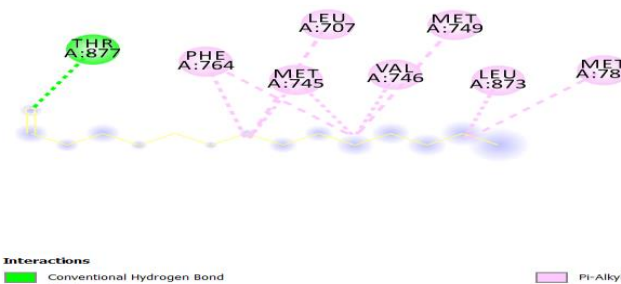
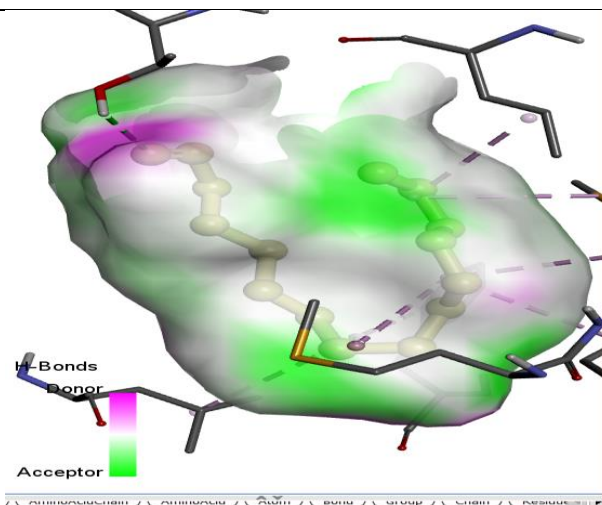


Interactions  
Conventional Hydrogen Bond  
Alkyl

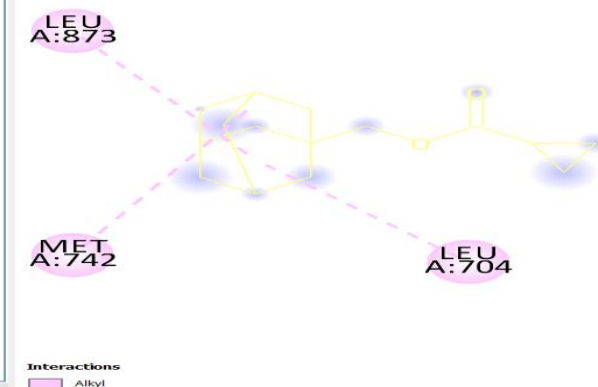
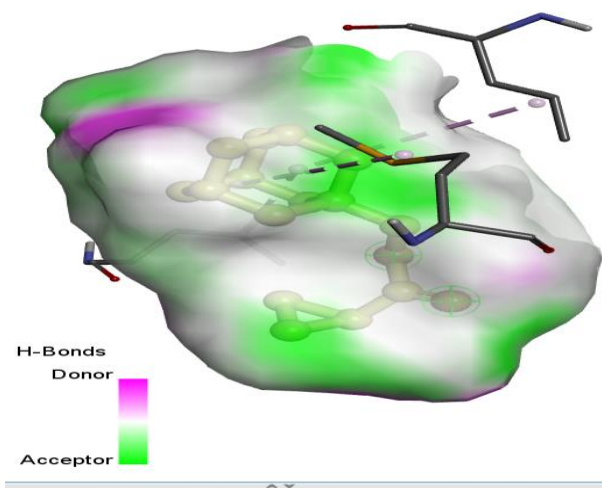
Pi-Alkyl



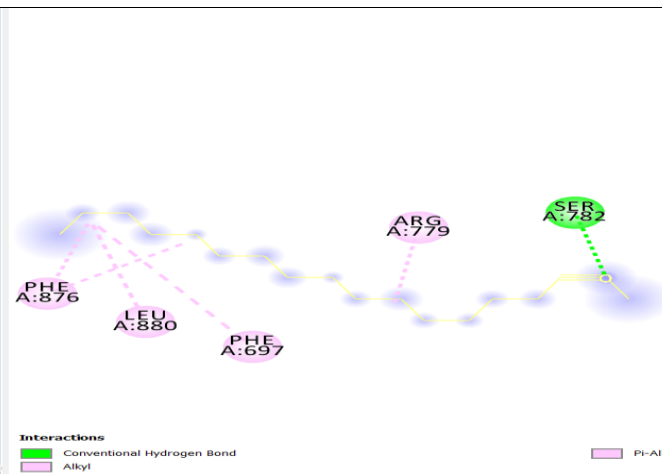
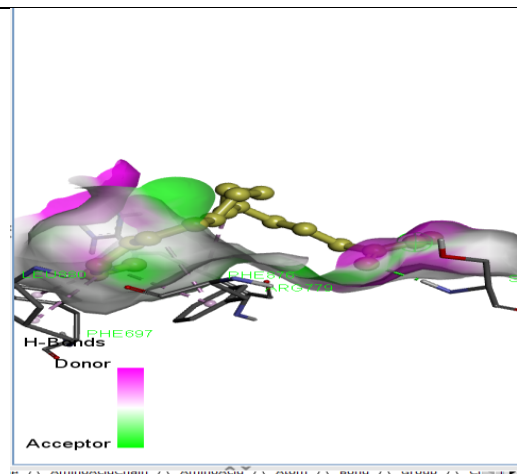
### Tetradecanal



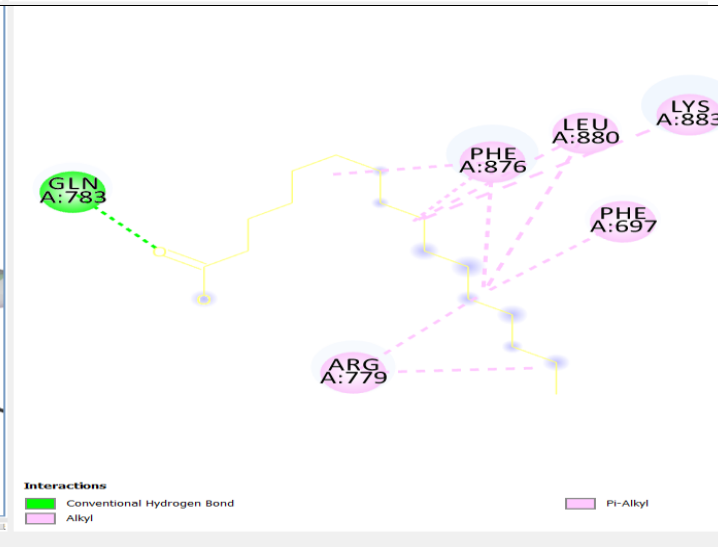
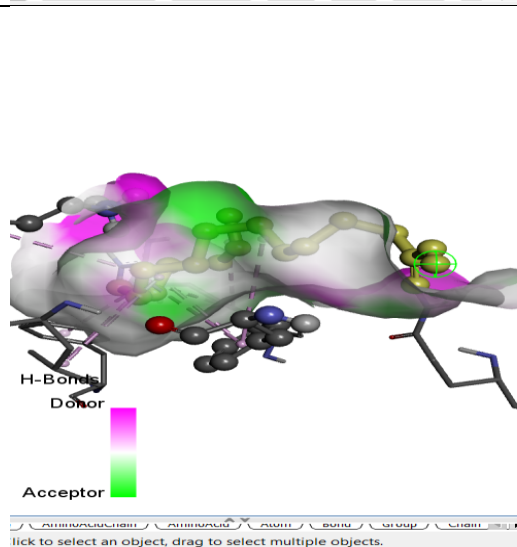
### Cyclopropanecarboxylic acid, (adamantanyl-1)methyl ester



### Hexadecanoic acid, methyl ester

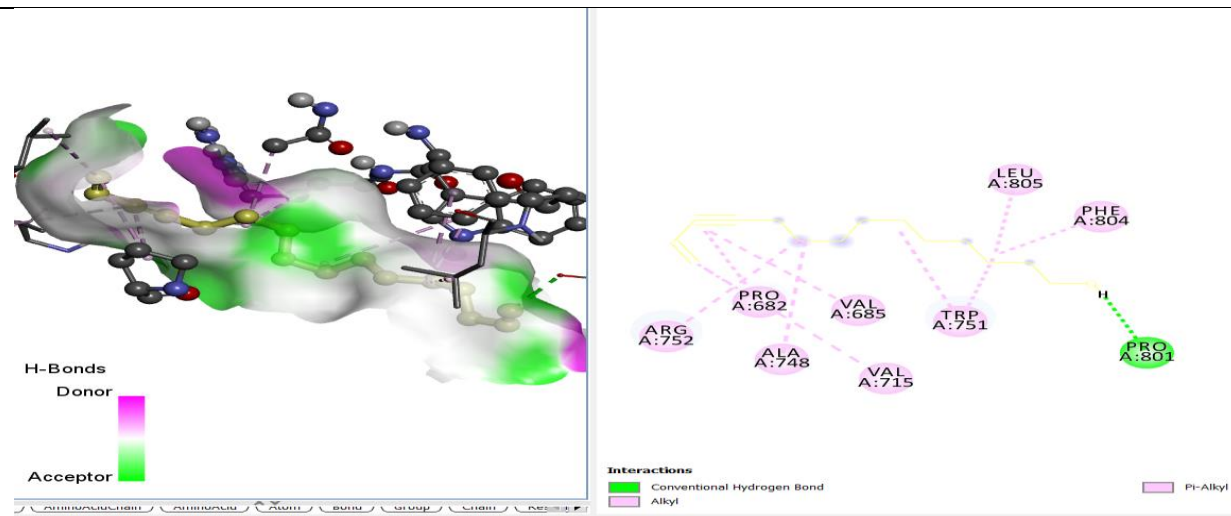


### n-Hexadecanoic acid

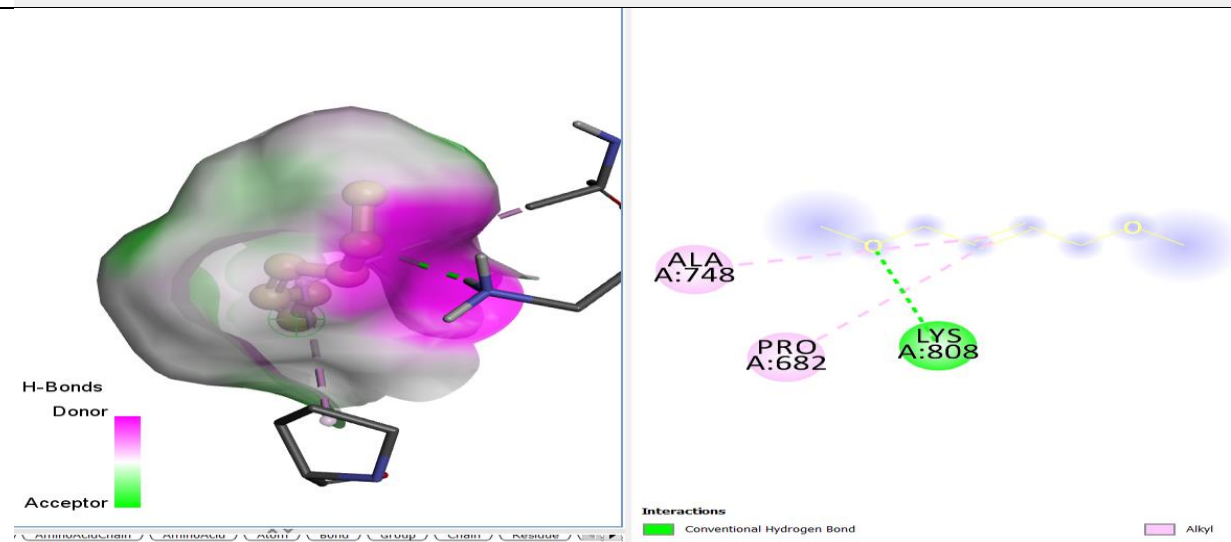


click to select an object, drag to select multiple objects.

### 13-Tetradecene-1-yn-1-ol

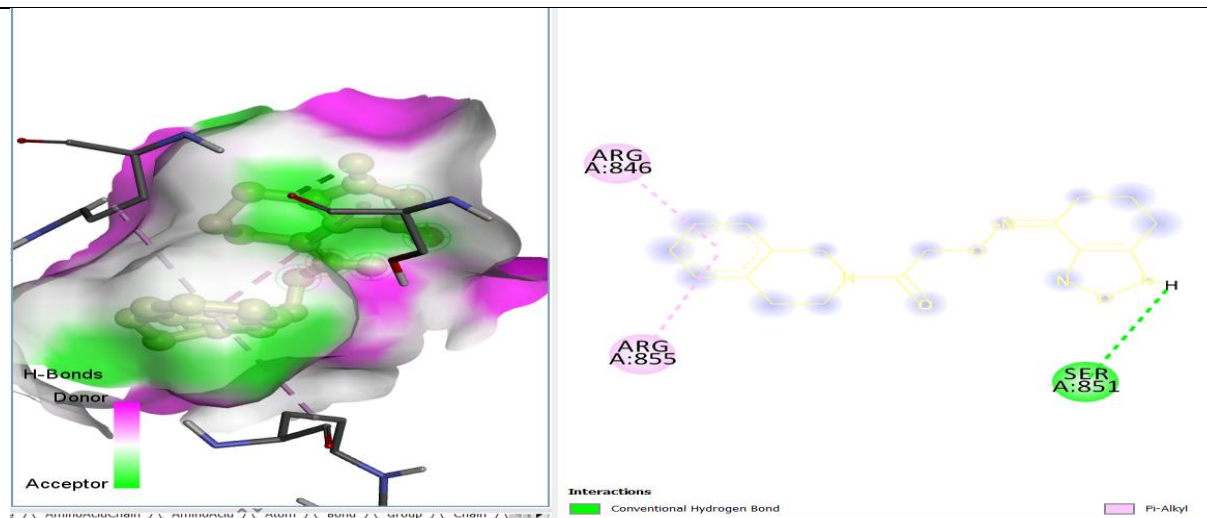


### 1,3-Butadiene, 1,4-dimethoxy-, (E,E)-

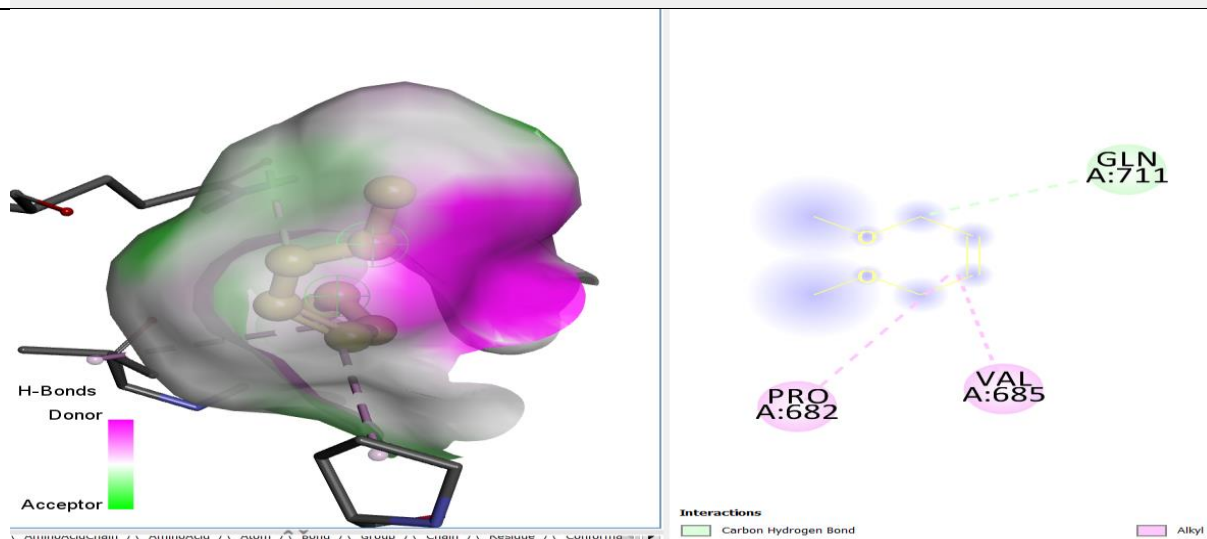




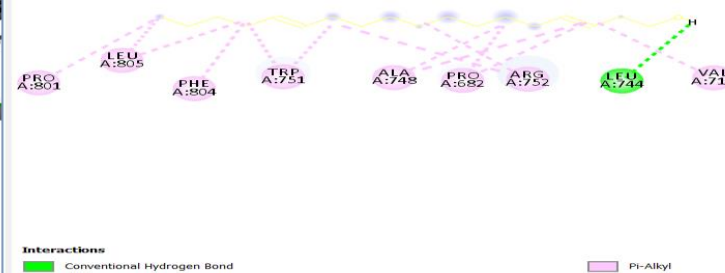
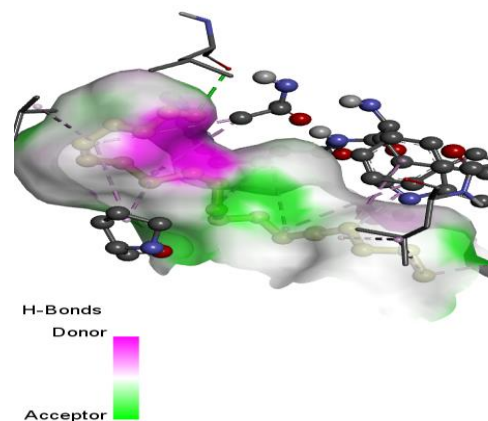
2,1,3-Benzoxadiazol-4(5H)-one, 6,7-dihydro-, O-[2-[3,4-dihydro-2(1H)-isoquinolinyl]-2-oxoethyl]oxime



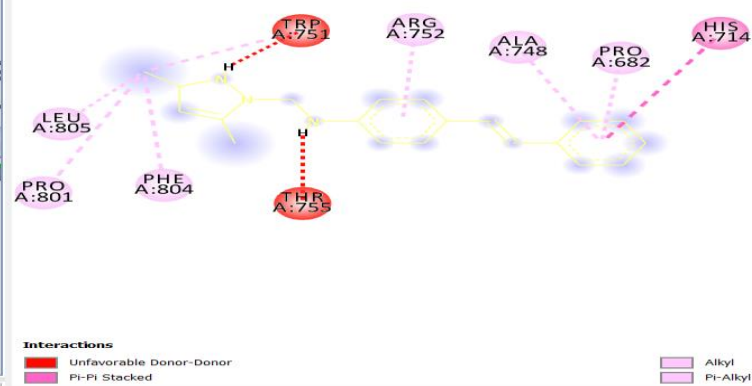
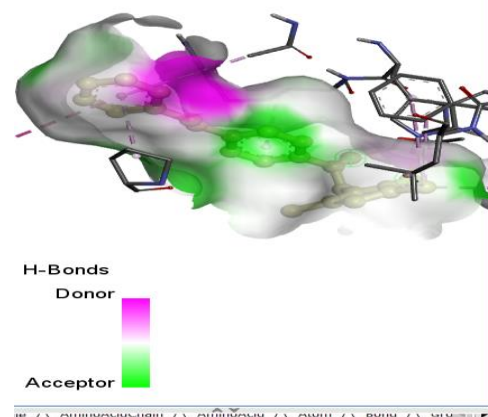
1,3-Butadiene, 1,4-dimethoxy-, (Z,Z)-



**Z,E-3,13-Octadecadien-1-ol**



**Benzenamine, 4-(2-phenylethenyl)-N-(3,5-dimethyl-1-pyrazolylmethyl)-**

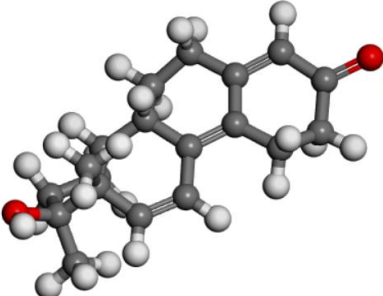
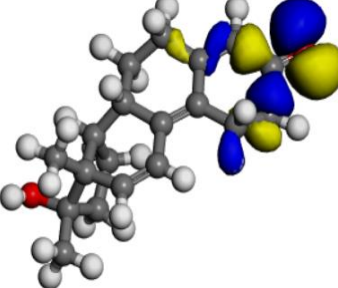
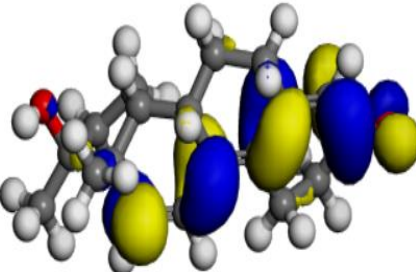
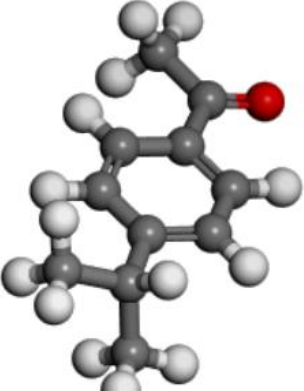
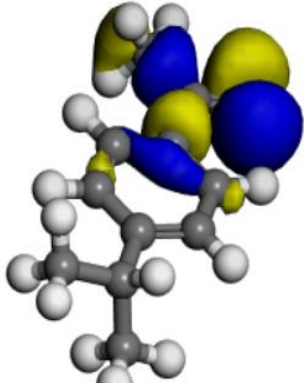
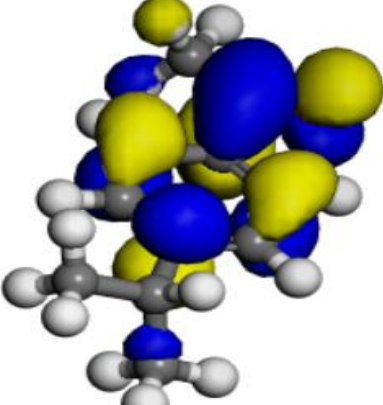
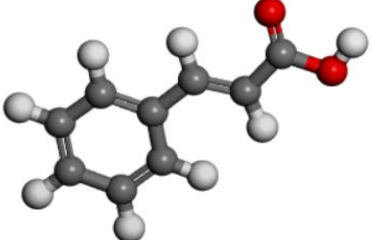
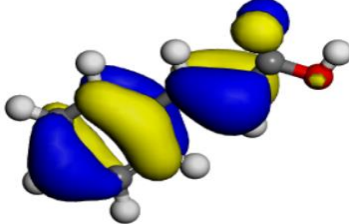
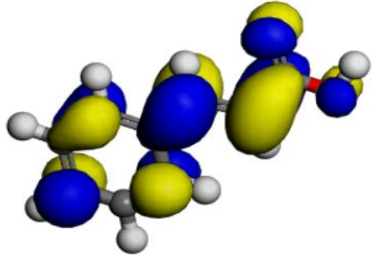


**Fig. 4. Target-ligand interactions of identified compounds**

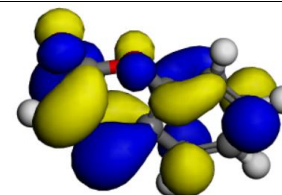
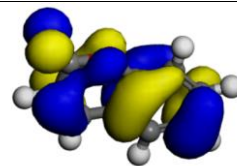
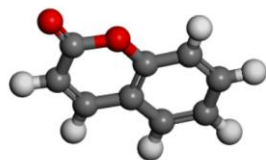
**Table 4. Amino acid residues and forces of interactions between the target and ligands**

S/no.	Compound	Amino acid involved	Type of interaction
1.	Methyltrienolone	TYR 915, SER 865	Unfavorable acceptor-acceptor, pi-alkyl, pi-sigma
2.	Ethanone, 1-[4-(1-methylethyl)phenyl]-	MET 780, LEU 704	Pi-sigma, pi-sulfur
3.	trans-Cinnamic acid	ALA748, PHE 764, PRO 682, VAL 685	Conventional hydrogen bond, unfavorable acceptor-acceptor, pi-alkyl
4.	Coumarin	ARG 752, GLN 711, LEU 704, MET 749, MET 745,	conventional hydrogen bond, pi-alkyl
5.	2-Carboxycinnamic acid	ASN 705, LEU 704, MET 745, MET 749, PHE 764	conventional hydrogen bond, pi-alkyl, Pi-sigma, pi-pi – shaped
6	Naphthalene, 1,2,4a,5,6,8a-hexahydro-4,7-dimethyl-1-(1-methylethyl)-	LEU 704, LEU 707, MET 745, MET 895, PHE 764, TRP 741, VAL 746	Alkyl, pi-alkyl
7	Benzene, 1-(1,5-dimethyl-4-hexenyl)-4-methyl-	LEU 880, PHE 697, PHE 876, LYS 883, VAL 887	Pi-cation, alkyl, pi-alkyl, pi-pi stacked
8	.alpha.-Muurolene	LEU 704, LEU 707, MET 745, MET 895, PHE 764, TRP 741, VAL 746	Alkyl, pi-alkyl
9	2-Propenal, 3-(2-methoxyphenyl)-	ASN 705, LEU 704, LEU707, MET 742, MET 745, MET 787PHE 764, VAL 746	carbon-hydrogen bond, alkyl, pi-alkyl, pi-sulfur, pi-sigma, pi-pi T-shaped
10	.alpha.-Calacorene	LEU 704, LEU 707, LEU 873, MET 745, MET 780, MET 787	Alkyl, pi-alkyl, pi-sigma
11	Cyclooctane, cyclohexyl-	LEU 704, LEU 873, MET 745, MET 780, PHE 764	Alkyl, pi-alkyl
12	Cyclohexane, 1-ethenyl-1-methyl-2-(1-methylethenyl)-4-(1-methylethylidene)-	LEU 704, MET 745	Alkyl
13	3-Cyclohexen-1-carboxaldehyde, 3,4-dimethyl-	LEU 704, MET 745,	alkyl, pi-alkyl
14	2H-Indazole, 2-methyl-4-nitro-	ARG 752, GLN 711 LEU 704, MET 745, MET 749, PHE 764,	conventional hydrogen, carbon hydrogen, pi-alkyl, pi-pi T-shaped
15	.tau.-Muurolol	LEU 704, LEU 873, MET 745, MET780, PHE 876	alkyl, pi-alkyl
16	Copaene	LEU 701, LEU 704, LEU 873, MET 780, PHE 764	Alkyl, pi-alkyl
17	Tricyclo[5.2.1.0 (2,6)]decan-10-ol	LEU 704, LEU 873, MET 745, MET 749, PHE 764	Alkyl, pi-alkyl
18	Benzaldehyde, 4-hydroxy-3,5-dimethoxy-	ALA 748, ARG 752, GLU 681, GLN 711, LYS 808, PRO 682, TRP 751, VAL 715	Conventional hydrogen bond, carbon hydrogen Alkyl, pi-alkyl, pi-cation
19	Naphthalene, 1,6-dimethyl-4-(1-methylethyl)-	ARG 778, LEU 880, LYS 883, PHE 879	Alkyl, pi-alkyl, pi-pi stacked

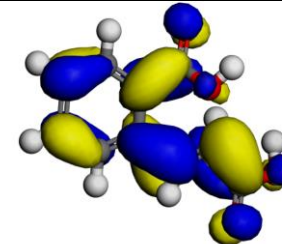
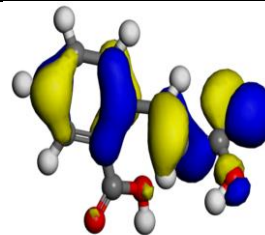
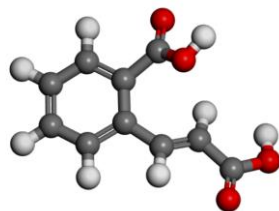
S/no.	Compound	Amino acid involved	Type of interaction
20	5,6-Dihydro-2-(4-tolyl)-4H-1,3-oxazin-5-one	AGR 752, GLN 711, LEU 701, LEU 704, MET 745, MET 780, PHE 876,	conventional hydrogen, carbon hydrogen, pi-alkyl, pi-sulfur, pi-sigma, pi-alkyl
21	5,6,7,8-Tetramethylbicyclo[4.1.0]hept-4-en-3-one	Nil	Nil
22	13-Octadecenal, (Z)-	ALA 748, ARG 752, PHE 804, PRO 682, TRP 751, VAL 715, VAL 684,	Conventional hydrogen bond, alkyl, pi-alkyl
23	Tetradecanal	LEU 707, LEU 873, MET 745, MET 749, MET 787, PHE 764, THR 877, VAL 746	Conventional hydrogen bond, alkyl, pi-alkyl
24	Cyclopropanecarboxylic acid, (adamantany-1)methyl ester	LEU 704, LEU 873, MET 742	Alkyl
25	Hexadecanoic acid, methyl ester	ARG 779, LEU 880, PHE 697, PHE 876, SER 782	Conventional hydrogen bond, alkyl pi-alkyl
26	n-Hexadecanoic acid	ARG 779, GLN 783, LEU 880, PHE 697, PHE 876, LYS 883	Conventional hydrogen bond, alkyl pi-alkyl
27	13-Tetradecene-11-yn-1-ol	ALA 748, ARG 752, LEU 805, PHE 804, PRO 682, PRO 801, TRP 751, VAL 685, VAL 715	Conventional hydrogen bond, alkyl, pi-alkyl
28	1,3-Butadiene, 1,4-dimethoxy-, (E,E)-	ALA 748, LYS 808, PRO 682	Conventional hydrogen bond, alkyl
29	2,1,3-Benzoxadiazol-4(5H)-one, 6,7-dihydro-, O-[2-[3,4-dihydro-2(1H)-isoquinoliny]-2-oxoethyl]oxime	AGR 846, AGR 855, SER 851	Conventional hydrogen bond, alkyl
30	1,3-Butadiene, 1,4-dimethoxy-, (Z,Z)-	GLN 711, PRO 682, VAL 685	Carbon hydrogen bond, alkyl
31	Z,E-3,13-Octadecadien-1-ol	ALA 748, ARG 752, LEU 744, LEU 805, PHE 804, PRO 682, PRO 801, TRP 751, VAL 715	Conventional hydrogen bond, alkyl, pi-alkyl
32	Benzenamine, 4-(2-phenylethenyl)-N-(3,5-dimethyl-1-pyrazolylmethyl)-	ALA 748, ARG 752, LEU 805, HIS 714, PHE 804, PRO 682, PRO 801, TRP 752, THR 755	Unfavorable donor-donor, alkyl, pi-alkyl, pi-pi stacked

Compound	Optimized structure	HOMO orbital	LUMO orbital
Methyltrienolone			
Ethanone, 1-[4-(1-methylethyl)phenyl]-			
trans-Cinnamic acid			

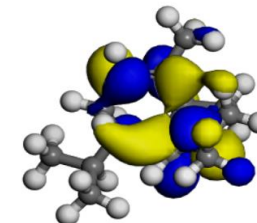
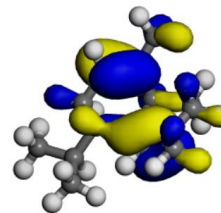
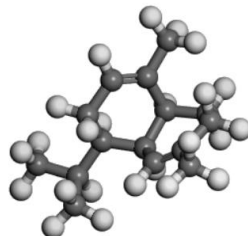
**Coumarin**



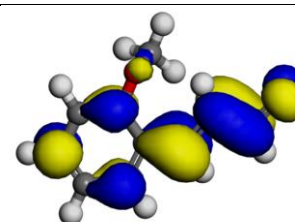
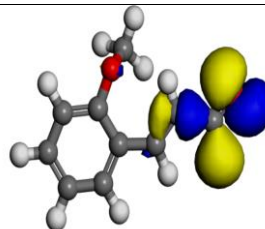
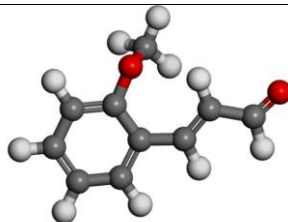
**2-Carboxycinnamic acid**



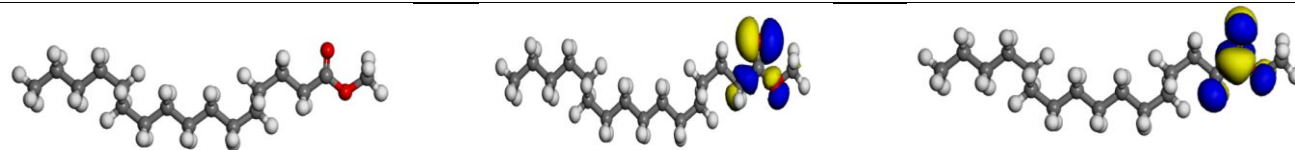
**alpha-Muurolene**



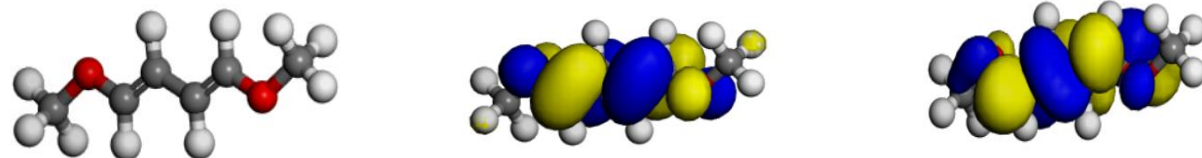
**2-Propenal, 3-(2-methoxyphenyl)-**



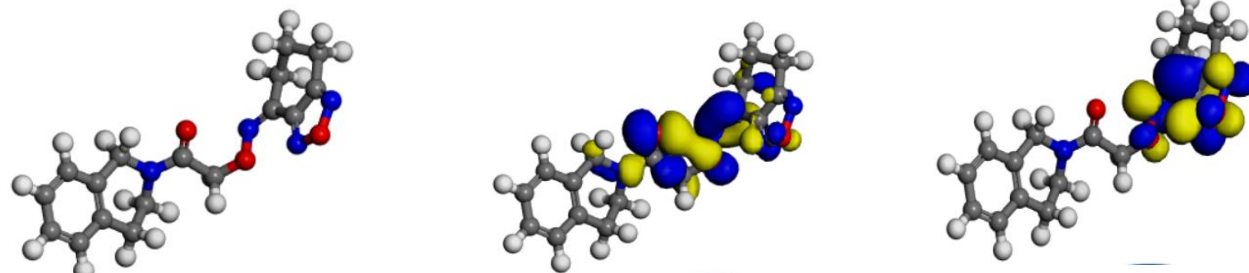
Hexadecanoic acid, methyl ester



1,3-Butadiene, 1,4-dimethoxy-, (E,E)-



2,1,3-Benzoxadiazol-4(5H)-one, 6,7-dihydro-, O-[2-[3,4-dihydro-2(1H)-isoquinoliny]-2-oxoethyl]oxime



Benzenamine, 4-(2-phenylethenyl)-N-(3,5-dimethyl-1-pyrazolylmethyl)-

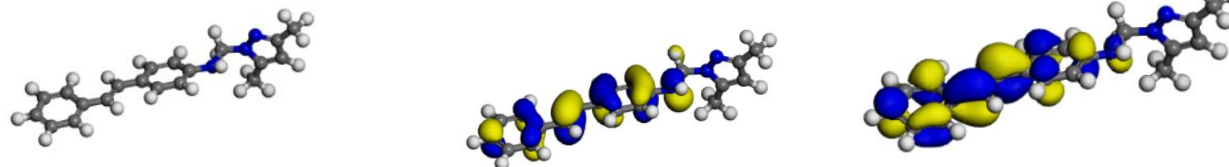


Fig. 5. density functional theory properties of some of the selected compounds, optimized structures, HOMO and LUMO orbitals. (atom legend: white-H, light gray-C and pink-O)

Table 5. Quantum chemical descriptor of the selected compounds

Compound	$E_{\text{HOMO}}$ (eV)	$E_{\text{OMO}}$ (eV)	$\text{IP} = -E_{\text{HOMO}}$	$\text{EA} = -E_{\text{LUMO}}$	Energy gap ( $E_{\text{LUMO}} - E_{\text{HOMO}}$ ) (eV)	$\chi$	$\eta$	$\delta$
Methyltrienolone	-5.0340	-2.8027	5.0340	2.8027	2.2313	3.9184	1.1157	0.8963
Ethanone, 1-[4-(1-methylethyl)phenyl]-	-5.5238	-2.3946	5.5238	2.3946	3.1292	3.9592	1.5646	0.6391
trans-Cinnamic acid	-6.0401	-2.8300	6.0401	2.8300	3.2101	4.4351	1.6051	0.6230
Coumarin	-6.0681	-2.8572	6.0681	2.8572	3.2109	4.4627	1.6055	0.6229
2-Carboxycinnamic acid	-6.3674	-3.2653	6.3674	3.2653	3.1021	4.8164	1.5511	0.6447
.alpha.-Muurolene	-5.1701	-0.2177	5.1701	0.2177	4.9524	2.6939	2.4762	0.4038
2-Propenal, 3-(2-methoxyphenyl)-	-5.5238	-3.0748	5.5238	3.0748	2.4490	4.2993	1.2245	0.8167
Hexadecanoic acid, methyl ester	-6.2857	-0.8245	6.2857	0.8245	5.4612	3.5551	2.7306	0.36621
1,3-Butadiene, 1,4-dimethoxy-, (E,E)-	-4.1360	-0.7612	4.1360	0.7612	3.3748	2.4486	1.6874	0.5926
2,1,3-Benzoxadiazol-4(5H)-one, 6,7-dihydro-, O-[2-[3,4-dihydro-2(1H)-isoquinolinyl]-2-oxoethyl]oxime	-5.5782	-2.4762	5.5782	2.4762	3.102	4.0272	1.5510	0.6447
Benzenamine, 4-(2-phenylethenyl)-N-(3,5-dimethyl-1-pyrazolylmethyl)-	-4.5170	-1.9591	4.5170	1.9591	2.5579	3.2381	1.2790	0.7819



### 3.3 Molecular Docking Data

Computational molecular docking study was performed to identify the target-ligand interaction effects between the chosen human androgen receptor (PDB:1e3g) and the identified compounds. The docking binding energies are shown in Table 3 while Fig. 4 shows the 3-dimensional (3D) and 2-dimensional (2D) protein-ligand interactions. Copaene gave the lowest binding score ( $-8.2 \text{ Kcal mol}^{-1}$ ), better than Methyltrienolone which was used as the control and gave binding energy of  $-6.8 \text{ Kcal mol}^{-1}$ .

The amino acids involved in the ligand-target interactions as well as the force of interactions involved are presented in Table 4. Major forces of interactions observed include Conventional hydrogen bond, unfavorable acceptor-acceptor, alkyl, pi-alkyl, Pi-cation, pi-pi stacked and pi-sigma.

### 3.4 Density Functional Theory Results

To ascertain the relationship between the structures of the compounds and their reactivity, density functional theory calculations were undertaken. The calculations were performed in the electronic structure DMol<sup>3</sup> program in the frame work of the Perdew-Wang (PW) local correlation density functional, Mulliken population analysis, and the DND basis set [27], geometric optimization was performed on the structures prior to frontier orbital calculations. The compounds with area peaks greater than 1 % in the GC-MS result were selected for the DFT studies. Fig. 5 shows the optimized structures and the frontier orbitals while Table 5 revealed the electronic properties of the compounds. The highest occupied molecular orbital (HOMO) and the lowest unoccupied molecular orbitals (LUMO) also known as the frontier molecular orbitals are employed in predicting the most reactive regions in a molecule, they are used in describing the chemical reactivity patterns of molecules [28], the HOMO orbital is rich in electron and has a tendency to donate to electron unoccupied region whereas the LUMO orbital is electron deficient region ready to accept from the electron rich environment, the gap energy (HOMO-LUMO) is related to the kinetic stability and chemical reactivity of the molecules studied [29] hence a molecule with small gap energy will show high polarizability and good chemical reactivity as well as low kinetic stability, and is qualified to be classified as a soft molecule. Using the HOMO and LUMO energies the quantum chemical descriptor including hardness ( $\eta$ ), softness ( $\delta$ )

and electronegativity ( $\chi$ ) were calculated with the equations below:

$$\chi = \frac{IP+EA}{2} \quad (1)$$

$$\eta = \frac{IP-EA}{2} \quad (2)$$

$$\delta = \frac{1}{\eta} \quad (3)$$

Where  $IP$  represents the ionization potential and  $EA$  is the electron affinity, the hardness shows the tendency of the compound to resist the transfer of electron, it is an indication of good chemical reactivity, the softness shows the tendency of a chemical compound to draw electron to its and the electronegativity shows the compounds ability to attract electron to itself when participating in a covalent bond system. The calculated values of the quantum chemical descriptors shown in Table 5 show that the compounds would have good reactivity towards the drug target.

## 4. CONCLUSION

The extract constituents of *Cinnamomum zeylanicum* were extracted in chloroform; FTIR examination performed on the sample showed that it contained some functional groups which are favorable for drug formulation. The GC-MS result revealed that the plant contained 31 compounds with favorable pharmacological and pharmacodynamics properties to humans. The molecular docking result using Methyltrienolone as control drug showed that copaene gave the lowest binding score ( $-8.2 \text{ k cal mol}^{-1}$ ) which is an indication that the compounds contained in the plant could be a good drug candidate for prostate cancer control. Density functional theory calculations were performed on some of the compounds identified in the GC-MS analysis and the low values of the energy gap confirmed the chemical reactivities of the molecules towards the drug target. Generally, the values of the calculated quantum chemical descriptors indicated that the compounds would be good drug lead candidates. Further findings are encouraged on the plant material which may include; the isolation and analysis of the compounds from the plant material as well as in-vivo /in-vitro screening to further validate the computational results.

### DISCLAIMER (ARTIFICIAL INTELLIGENCE)

Author(s) hereby declare that NO generative AI technologies such as Large Language Models

(ChatGPT, COPILOT, etc) and text-to-image generators have been used during writing or editing of manuscripts.

## COMPETING INTERESTS

Authors have declared that no competing interests exist.

## REFERENCES

1. Jimmy CL, Stephanie CE. Prostate Gland, Encyclopedia of Reproduction (Second Edition), 201 Textbook of Veterinary Diagnostic Radiology (Seventh Edition); 2018.
2. Jemal A, Center M M, DeSantis C, Ward E M. Global patterns of cancer incidence and mortality rates and trends. *Cancer Epidemiology, Biomarkers & Prevention*. 2010;19(8):1893-907.
3. Mattiuzzi C, Lippi G. Current cancer epidemiology. *Journal of epidemiology Global Health.*; 2019;9(4):217-222.
4. Bray F, Ferlay J, Soerjomataram I, Siegel R, Torre L, Jemal A. Global cancer statistics: GLOBOCAN estimates of incidence and mortality worldwide for 36 cancers in 185 countries. *CA Cancer Journal of Clinicians*. 2018;68(6):394 – 424.  
Available:<https://doi.org/https://doi.org/10.3322/caac.21492>
5. Li Y, Ahmad A, Kong D, et al. Recent progress on nutraceutical research in prostate cancer. *Cancer Metastasis Revelation*. 2014;33(2–3):629–640.  
DOI: 10.1007/s10555-013-9478-9
6. Pendleton J M, Tan W W, Anai S. Phase II trial of isoflavone in prostate-specific antigen recurrent prostate cancer after previous local therapy. *BMC Cancer*. 2008; 8:132–2407-8–132 .  
DOI: 10.1186/1471-2407-8-132.
7. Tavsan Z, Kayali HA. Flavonoids showed anticancer effects on the ovarian cancer cells: involvement of reactive oxygen species, apoptosis, cell cycle and invasion. *Biomedical Pharmacother*. 2019;116: 109004
8. Faezeh T, Shahin A, Shahram L, Parvin K, Ali A, In-silico activity prediction and docking studies of some flavonoid derivatives as anti-prostate cancer agents based on Monte Carlo optimization. *BMC Chemistry*. 2023;17:87.
9. Ranasinghe P, Pigera S, Premakumara GA, Galappaththy P, Constantine G R, Katulanda P. Medicinal properties of 'true' cinnamon (*Cinnamomum zeylanicum*): a systematic review. *BMC Complementary and alternative Medicine*. 2013;2213:275. DOI: 10.1186/1472-6882-13-275. PMID: 24148965; PMCID: PMC3854496.
10. Pallavi K, Rathai R, Cinnamon: Mystic powers of a minute ingredient, *Pharmacognosy Research*. 2015;7,
11. Reichard P, Nilsson BY, Rosenqvist U. The effect of long-term intensified insulin treatment on the development of microvascular complications of diabetes mellitus. *N England Journal of Medicine*. 1993;329:304-9.
12. Skyler JS. Effects of glycemic control on diabetes complications and on the prevention of diabetes. *Clinical Diabetes*. 2004;22:162-6.
13. Han DC, Lee MY, Shin KD, Jeon SB, Kim JM, Son KH. 2'-benzoyloxycinnamaldehyde induces apoptosis in human carcinoma via reactive oxygen species. *Journal of Biological Chemistry*. 2004;279(69):11-20.
14. Kwon HK, Jeon WK, Hwang JS, Lee CG, So JS, Park JA. Cinnamon extract suppresses tumor progression by modulating angiogenesis and the effector function of CD8+ T cells. *Cancer Letters* 2009;278:174-82.
15. Meng XY, Zhang HX, Mezei M, Cui M, Molecular docking: A powerful approach for structure-based drug discovery. *Current Computational Aided Drug Des*. 2011; 7(2):46-57.  
DOI: 10.2174/157340911795677602  
PMID: 21534921; PMCID: PMC3151162.
16. Agu PC, Afiukwa CA, Orji OU. Molecular docking as a tool for the discovery of molecular targets of nutraceuticals in diseases management. *Scientific reports*. 2023;13:13398.  
Available:<https://doi.org/10.1038/s41598-023-40160-2>
17. Sahoo RN, Pattanaik S, Pattnaik G, Mallick S, Mohapatra R, Review on the use of molecular docking as the first line tool in drug discovery and development. *Indian Journal of Pharmaceutical Sciences*. 2022; 84(5):1334–1337.
18. Jain AN, Virtual screening in lead discovery and optimization. *Current Opinion in Drug Discovery and Development*. 2004;7(4):396–403.
19. Ikpa CBC, Ikezu UJM, Maduwuba MC, *In silico* docking analysis of anti-malaria and

- anti-typhoid potentials of phytochemical constituents of ethanol extract of dryopteris dilatata, Tropical Journal of Natural Product Research. 2022;6(5):772-782.
20. Adindu CB, *In-silico* screening of lung cancer inhibiting potential of the chemical constituents of N-Hexane Extract of Elaisi guineenses, Journal of Materials Science Research and Reviews. 2023;6(3):572-582.
  21. Arthur MN, Bebla K, Broni E, Ashley C, Velazquez M, Hua X, Radhakrishnan R, Kwofie S K, Miller WA, Design of Inhibitors That Target the Menin–Mixed-Lineage Leukemia Interaction. Computation. 2024; 12(1):3.  
Available:<https://doi.org/10.3390/computati on12010003>
  22. Singh AN, Baruah MM, Sharma N. Structure based docking studies towards exploring potential anti-androgen activity of selected phytochemicals against prostate cancer. Scientific Reports. 2017;16:7(1) :1955.  
DOI: 10.1038/s41598-017-02023-5.  
PMID: 28512306; PMCID: PMC5434041.
  23. Pedro MM. Structural evidence for ligand specificity in the binding domain of the human androgen receptor, implications for pathogenic gene mutations. Journal of Biological Chemistry. 2000;275(34):2616 4-26171.
  24. Sujana D, Sumiwi SA, Saptarini NM, Levita J, Admet prediction and molecular docking simulation of phytoconstituents in *Boesenbergia rotunda* rhizome with the effector caspases to understand their protective effects, Rasayan Journal of Chemistry. 2022;15(4):2401-2406.
  25. Tripathi D, Koora S, Satyanarayana K, Saleem Basha S, Jayaraman S. Molecular docking analysis of COX-2 with compounds from Piper longum. Bioinformation. 2021;17(6):623-627.  
DOI: 10.6026/97320630017623.  
PMID: 35173384; PMCID: PMC8819790.
  26. Rahul T, Bruce AR, Makedonka M. *In silico* Drug Design, Academic Press. 2019;329-358,  
Available:<https://doi.org/10.1016/B978-0-12-816125-8.00012-2>
  27. Oguzie EE, Ogukwe CE, Ogbulie JN, Nwanebu FC, Adindu CB, Udeze IO, Oguzie KL, Eze FC. Broad spectrum corrosion inhibition: corrosion and microbial (SRB) growth inhibiting effects of *Piper guineense* extract, Journal of Material Science. 2012;(47): 3592–360.
  28. Hussein RK, Elkhair HAO, Ilnaouf KH. Spectral, structural, stability characteristics and frontier molecular orbitals of tri-n-butyl phosphate (tbp) and its Degradation Products: DFT calculations. J. Ovonic Res. 2021;17:23–30.
  29. Rauk A. Orbital interaction keory of organic chemistry, 2nd edition, Wiley-Interscience, Hoboken, NJ, USA. 2001;86.

**Disclaimer/Publisher's Note:** The statements, opinions and data contained in all publications are solely those of the individual author(s) and contributor(s) and not of the publisher and/or the editor(s). This publisher and/or the editor(s) disclaim responsibility for any injury to people or property resulting from any ideas, methods, instructions or products referred to in the content.

© Copyright (2024): Author(s). The licensee is the journal publisher. This is an Open Access article distributed under the terms of the Creative Commons Attribution License (<http://creativecommons.org/licenses/by/4.0>), which permits unrestricted use, distribution, and reproduction in any medium, provided the original work is properly cited.

Peer-review history:

The peer review history for this paper can be accessed here:

<https://www.sdiarticle5.com/review-history/120835>